CERN-EP-2020-004
2020/04/22

CMS-HIG-19-004

A measurement of the Higgs boson mass in the diphoton decay channel

The CMS Collaboration*

Abstract

A measurement of the mass of the Higgs boson in the diphoton decay channel is presented. This analysis is based on 35.9 fb^{-1} of proton-proton collision data collected during the 2016 LHC running period, with the CMS detector at a center-of-mass energy of 13 TeV. A refined detector calibration and new analysis techniques have been used to improve the precision of this measurement. The Higgs boson mass is measured to be $m_{\mathrm{H}} = 125.78 \pm 0.26\,\mathrm{GeV}$. This is combined with a measurement of m_{H} already performed in the $\mathrm{H} \to \mathrm{ZZ} \to 4\ell$ decay channel using the same data set, giving $m_{\mathrm{H}} = 125.46 \pm 0.16\,\mathrm{GeV}$. This result, when further combined with an earlier measurement of m_{H} using data collected in 2011 and 2012 with the CMS detector, gives a value for the Higgs boson mass of $m_{\mathrm{H}} = 125.38 \pm 0.14\,\mathrm{GeV}$. This is currently the most precise measurement of the mass of the Higgs boson.

"Published in Physics Letters B as doi:10.1016/j.physletb.2020.135425."

arXiv:2002.06398v2 [hep-ex] 21 Apr 2020

*See Appendix A for the list of collaboration members

1 Introduction

The independent observations of the Higgs boson by the ATLAS and CMS Collaborations [1–3] in proton-proton collisions at the CERN LHC was a key milestone in the understanding of the mechanism of electroweak symmetry breaking. More recently, with the increased amount of data resulting from the higher energy and the higher luminosity accumulated at the LHC between 2015 and 2018 (Run 2), the focus has shifted from observation to precision measurements of its properties. The couplings of the Higgs boson to other elementary particles can be predicted by the standard model of particle physics once its mass is known. This motivates precise measurements of the mass of the Higgs boson (m_{H}) in all available decay channels.

Although the $\mathrm{H} \to \gamma\gamma$ decay channel has a small (≈0.23%) branching fraction, it provides a clean final state topology in which the diphoton invariant mass can be reconstructed with high precision. The measurement of m_{H} in this decay channel can be combined with measurements in other decay channels to achieve an even higher precision. In this way the ATLAS and CMS Collaborations measured m_{H} to be $125.09 \pm 0.24\,\mathrm{GeV}$ [4] with the data collected in 2011 and 2012 (Run 1).

In this Letter, we present a new measurement of m_{H} in the $\mathrm{H} \to \gamma\gamma$ decay channel with the data collected at $\sqrt{s} = 13\,\mathrm{TeV}$ in 2016 corresponding to an integrated luminosity of $35.9\,\mathrm{fb}^{-1}$. The CMS Collaboration has previously reported a measurement of m_{H} with the same data set in the $\mathrm{H} \to \mathrm{ZZ} \to 4\ell$ decay channel where m_{H} was measured to be $125.26 \pm 0.21\,\mathrm{GeV}$ [5]. The ATLAS collaboration have also published a measurement of m_{H} of $124.97 \pm 0.24\,\mathrm{GeV}$ [6], using the combined 2016 and Run 1 data sets. Our measurements of m_{H} with the 2016 data set, in the $\mathrm{H} \to \gamma\gamma$ and $\mathrm{H} \to \mathrm{ZZ} \to 4\ell$ decay channels, have been combined with our measurement of m_{H} with the Run 1 data set. The combined result and the procedure followed for this combination are also described in this Letter.

2 The CMS detector

The central feature of the CMS detector is a superconducting solenoid of 6 m internal diameter with a uniform magnetic field of 3.8 T. Inside the magnet volume are silicon pixel and strip trackers, a lead tungstate crystal electromagnetic calorimeter (ECAL), and a brass and scintillator hadron calorimeter, each composed of a barrel and two endcap sections. Gas-ionization chamber based muon detectors are embedded in the steel flux-return yoke outside the solenoid. The ECAL is a hermetic homogeneous calorimeter made of 61 200 lead tungstate ($\mathrm{PbWO_4}$) crystals mounted in the central barrel part, closed by 7324 crystals in each of the two endcaps. In the region $1.65 < |\eta| < 2.6$ a three-radiation-length-thick preshower detector with two orthogonal layers of silicon strips is placed in front of the endcap crystals. Avalanche photodiodes are used as photodetectors in the barrel and vacuum phototriodes in the endcaps. The barrel part of the ECAL (EB) covers the pseudorapidity range $|\eta| < 1.479$, while the endcap calorimeters cover the range $1.479 < |\eta| < 3.0$. A calorimeter with longitudinal quartz fibres complements the coverage provided by the barrel and endcap detectors. The first level of the CMS trigger system [7] uses information from the calorimeters and muon detectors to select the most interesting events in a fixed time interval of less than $4\,\mu\mathrm{s}$. The high-level trigger processor farm further decreases the event rate from around 100 kHz to around 1 kHz before data storage. A more detailed description of the CMS detector, together with a definition of the coordinate system and the relevant kinematic variables, can be found in Ref. [8].

3 Analysis strategy

The general strategy followed in this analysis is the same as that adopted in an earlier analysis by the CMS Collaboration of the Higgs boson properties in the diphoton channel [9]. Since that publication, refinements were made to increase the precision of the measurement of m_{H} through a better understanding of the systematic uncertainties of the measurement, and a more accurate detector calibration was performed. We have also improved the method, first introduced in Ref. [10], to measure and correct for nonlinear discrepancies in the energy scale with transverse momentum (p_{T}), of electrons from Z boson decay, between data and simulation by increasing the granularity of the correction. In addition, we have developed a method to evaluate the systematic uncertainty of the photon energy scale due to radiation damage of the ECAL crystals, and a simplified event categorisation, described in Section 6, is followed in the analysis.

With the new calibration, the detector response is more stable with time, leading to a reduction of the uncertainties in the corrections to the photon energy due to the material upstream of the ECAL and of the uncertainties associated with variables which describe the electromagnetic shower.

4 Data and simulation

The events used in this analysis were collected in 2016 with an integrated luminosity of 35.9 fb^{-1}. They were selected with a diphoton trigger that had asymmetric p_{T} thresholds of 30 and 18 GeV. Full details of the trigger selection and the measurement of the trigger efficiency can be found in Ref. [9]. To model the signal and background processes, events are generated with Monte Carlo techniques. The detailed response of the CMS detector is simulated using the GEANT4 package [11].

Signal events are simulated with the MADGRAPH5_aMC@NLO v2.2.2 matrix-element generator [12] at next-to-leading order and interfaced with PYTHIA 8.205 [13] for parton showering and hadronization. The PYTHIA underlying event tune CUETP8M1 [14] was used. The irreducible prompt diphoton background and the reducible backgrounds of γ + jet and multijet events, where the jets are misidentified as isolated photons, are the dominant backgrounds to the $\mathrm{H} \to \gamma\gamma$ decay process. The diphoton background is modelled with the SHERPA v.2.2.1 [15] generator, which includes the Born processes with up to 3 additional jets at leading order (LO) accuracy, as well as the LO box processes. The γ+jets and multijet backgrounds are modelled with PYTHIA at LO. These samples are used for the training of the multivariate discriminants used in this analysis, as well as for the optimisation of the event categorisation. The Drell–Yan samples used to derive the electron and photon energy scale corrections and their systematic uncertainties, are simulated with MADGRAPH [16] and MADGRAPH5_aMC@NLO generators and merged together in order to improve the statistical precision of the scale corrections. Before merging these samples, the compatibility of the m_{ee} lineshapes between the two generators in the categories used to derive the electron and photon energy scale corrections was confirmed.

The simulation includes multiple proton-proton interactions taking place within a bunch crossing, known as ‘pileup’. Pileup can occur not only in the same bunch crossing (in-time pileup), but also in the crossing of previous and subsequent bunches (out-of-time pileup), both of which are accounted for by the simulation. The simulated events are scaled to reproduce the distribution of the number of pileup interactions in data.

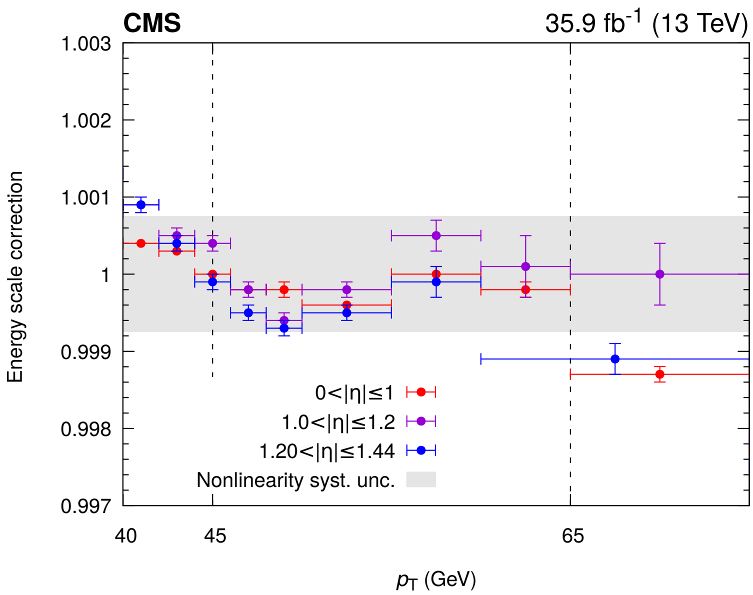

Figure 1: Energy scale corrections as a function of the p_T of the photon. The horizontal bars in the plot represent the variable bin width. The systematic uncertainty associated with this correction is approximately the maximum deviation observed in the p_T range between 45 and 65 GeV for electrons in the EB region.

5 Photon reconstruction and identification

Photon candidates are reconstructed as energy deposits in a collection of crystals in the ECAL. A cluster is formed by first identifying a 'seed' crystal with an energy above a given threshold, then the cluster is built by finding the crystals that share an edge with the seed crystal and have an energy above another, lower threshold. This second threshold is set to be approximately 80 MeV in the barrel and ranging from 80 to 300 MeV in the endcaps, depending on $|\eta|$. These clusters, once formed, are combined to form a 'supercluster', aiming to fully contain the shower of the photon. This procedure accounts for variations in geometry as a function of $|\eta|$, and optimises the robustness of the energy resolution against pileup.

5.1 Photon energy calibration

A critical component of the measurement of m_H is the energy calibration of the response of the ECAL to photons. The energy of a photon is calculated by summing the calibrated and corrected energy [17] of all crystals in the associated supercluster, and the energy deposited in the preshower in the region $1.65 < |\eta| < 2.6$ covered by this detector. For each supercluster, a shower shape variable R_9 is defined, which is used to select photons undergoing a conversion in the material between the interaction point and the front face of the ECAL. The variable R_9 is defined for a candidate electromagnetic cluster as the ratio of the sum of energy deposited in a 3×3 crystal array, centred on the crystal with the highest energy, to the sum of the energy in the supercluster. The energy deposition of photons that convert before reaching the calorimeter tends to have wider transverse profiles and thus lower values of R_9 than those of unconverted photons. To further optimise the energy resolution, the energy is corrected for the lack of complete containment of the electromagnetic showers in the clustered crystals, the energy lost by photons that convert upstream of the calorimeter, and the effects of pileup. These corrections are derived using a multivariate regression technique, trained on simulated events, which simultaneously estimates the energy of the photon and its median uncertainty. The inputs to this

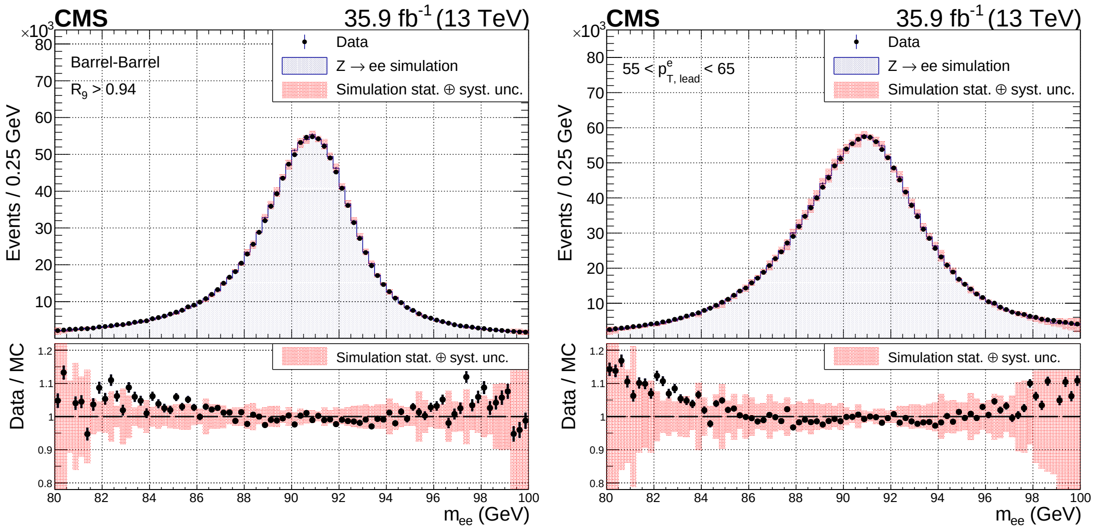

Figure 2: Comparison of the distributions of the invariant mass of the dielectrons in data and simulation in $Z \to ee$ events after application of energy corrections in two representative categories. Left: Both electrons are in the EB and satisfy $R_9 > 0.94$. Right: the leading electron has a transverse momentum between 55 and 65 GeV, without a requirement on the second electron. The systematic uncertainty in the error band in the plots include only the uncertainties on the derived energy scale corrections.

regression are shower shape variables, the preshower information, and observables sensitive to pileup [18].

After applying these corrections to the photon energy, some residual differences remain between the data and simulation in both the photon energy scale and the resolution. A multistep procedure is used to correct these differences, using $Z \to ee$ decays in which the electron showers are reconstructed as photons, so that the simulation accurately reproduces the data. In the first step of this process, any residual long-term drifts in the energy scale in data are corrected for, in approximately 18-hour intervals corresponding to one LHC fill. In the second step, corrections to both the energy resolution in the simulation, and the scale correction needed for the data are derived simultaneously in bins of $|\eta|$ and R_9 for electrons. The energy resolution obtained in simulation is matched to the data by adding a Gaussian smearing term, determined by adjusting the agreement in the $Z \to ee$ invariant mass distributions. In the third and final step the energy scale corrections are derived in bins of $|\eta|$ and p_T to account for any nonlinear response of the crystals with energy. The corrections obtained from this step are shown in Fig. 1 for electrons as a function of p_T in the three bins of $|\eta|$ in EB. This additional step in the scale correction improves the precision of the measurement of m_H, since the energy spectrum of the electrons from Z boson decay ($\langle p_T \rangle \approx 45$ GeV) used to derive the scale corrections, is different from the energy spectrum of photons from Higgs boson decay ($\langle p_T \rangle \approx 60$ GeV).

We note that in the second step the number of bins in R_9 for the scale corrections has been increased by a factor of five over the previous analysis [9], resulting in an improvement in the precision with which the energy scale is determined. Also, in order to provide a consistency test of the derivation procedure, the correction factors that are obtained in the second and third steps are applied a second time to the data and a new set of factors is extracted in the same electron categories. Any deviation from unity is an indication of the nonclosure of the derivation procedure and is applied as a systematic uncertainty on scale corrections.

The agreement between data and simulation in the dielectron invariant mass, after applying these energy scale corrections and the additional smearings, is shown in Fig. 2 for dielectron events in the EB with R_9 greater than 0.94, and for dielectron events with a leading transverse momentum between 55 and 65 GeV, without a requirement on the second electron. The former demonstrates the performance of the energy corrections on photons with the highest event count, optimal resolution, and the highest sensitivity to the Higgs boson mass. The latter demonstrates that the energy corrections are effective in a kinematic region where the p_T of the electron has been chosen to be the typical p_T of a photon from a Higgs boson decay. In both cases data and simulation are in good agreement in the core of the distributions.

5.2 Photon preselection and identification

The photons considered in the subsequent steps of this analysis are required to satisfy certain preselection criteria that are similar to, but more stringent than, those imposed by the trigger requirements. A detailed description of these preselection criteria, as well as the methods employed to evaluate their efficiencies, can be found in Ref. [9]. A dedicated boosted decision tree (BDT) is used to classify prompt photons from other photon candidates that arise out of misidentified jet fragments, but which satisfy the preselection criteria. The full details of the input features of this photon identification BDT is also described in Ref. [9]. The score of this BDT is used later in the event categorization, discussed in the next section.

5.3 Vertex selection

The identification of the diphoton vertex position along the beam axis has a direct impact on the diphoton mass resolution, since if the vertex position is known to better than about 1 cm, then the invariant mass resolution is dominated by the photon energy resolution. The distribution of the position of the interaction vertices along the beam axis has an RMS spread of about 3.4 cm, and, in typical pileup conditions in 2016, there were on average around 23 interactions in each bunch crossing. The choice of the diphoton vertex is made following the same procedure in Ref. [9]: a BDT, whose inputs are observables related to tracks recoiling against the diphoton system, is used to identify the most likely vertex. A second BDT is used to determine the probability of correctly choosing that vertex. The score of the second BDT is used later in the event categorisation, discussed below. The algorithm is validated using $Z \to \mu^+\mu^-$ events with the muon tracks removed so as to mimic diphoton pair production. The efficiency of assigning the event to a vertex within 1 cm of the true vertex in the simulated $H \to \gamma\gamma$ events is found to be approximately 81%.

6 Event classification

The event selection procedure is similar to that in Ref. [9]. The p_T of the two leading photons ($p_T^{\gamma 1}$, $p_T^{\gamma 2}$) are required to satisfy $p_T^{\gamma 1} > m_{\gamma\gamma}/3$ and $p_T^{\gamma 2} > m_{\gamma\gamma}/4$, where $m_{\gamma\gamma}$ is the diphoton mass, and the photon p_T requirement is applied after the vertex assignment. Additionally $m_{\gamma\gamma}$ is required to be between 100 and 180 GeV. The use of p_T thresholds scaled with the diphoton invariant mass is to prevent a distortion of the lower end of the invariant mass spectrum. The superclusters of both photons are required to have $|\eta| < 2.5$ and to be outside of the barrel-endcap transition region, $1.44 < |\eta| \leq 1.57$.

To improve the sensitivity of the analysis, events are classified according to their production mechanism, mass resolution, and their predicted signal-to-background ratio. A dedicated classifier, referred to as the diphoton BDT, is used to discriminate between signal and background events. This BDT assigns a high score to events with photons exhibiting signal-like kinematics, a good mass resolution, and a high score from the photon identification BDT. The per-event probability estimate of assigning the correct primary vertex to the diphoton system is used as one of the input features of this diphoton BDT. The other input features are described in Ref. [9].

Nearly 95% of Higgs boson events come from two production modes. These are gluon-gluon fusion (ggH) and vector boson fusion (VBF), where there are two jets in the final state separated by a large rapidity gap. A multivariate discriminant is trained to discriminate VBF events from ggH+ jets events, using the kinematics of the characteristic VBF dijet system as inputs. This discriminant is then given as an input to an additional multivariate classifier (VBF combined BDT) along with the score from the diphoton BDT, and the ratio $p_{\mathrm{T}}^{\gamma\gamma}/m_{\gamma\gamma}$. The VBF events are subdivided into three categories based on the VBF combined BDT score. The remaining events are mostly ggH events and are designated as 'untagged'. These events are further subdivided into four categories based on their diphoton BDT score.

Adding other possible analysis categories, where for example, the Higgs boson is produced in association with a vector boson, or with a pair of top quarks, adds only a small increment to the precision of the mass measurement at the cost of a significant increase in the analysis complexity. Thus, unlike in the earlier analysis [9], these production modes are not considered as separate categories in this analysis.

7 Signal and background models

In order to extract m_{H}, signal and background models are constructed to fit the diphoton mass distributions observed in the data. The signal models are derived using simulated Higgs boson events, while the background models used in the fits of the $m_{\gamma\gamma}$ spectra are derived directly from data.

7.1 Signal model

The resolution of m_{H} in the diphoton decay channel depends on the production mechanism and the analysis category. Hence the signal shapes used to model the diphoton invariant mass distributions are derived for every analysis category and with a nominal value for m_{H}, using simulated events from the different production modes. The simulation accounts for the trigger, reconstruction, and identification efficiencies, which are measured with data-driven techniques. A weight is applied to the simulated events so that the distribution of the number of interactions per bunch crossing and the location of the primary vertex are matched to the distributions observed in data. A detailed description of each of these steps can be found in Ref. [9].

Since the distribution of $m_{\gamma\gamma}$ depends on the correct assignment of the vertex associated with the diphoton candidate, signal models were constructed with correct and wrong vertex assignment scenarios separately. For each process, analysis category, and vertex scenario, the $m_{\gamma\gamma}$ distributions were fit with a sum of, at most, four Gaussian functions.

For each process, analysis category, and vertex scenario, a simultaneous fit of the signal samples at mass values ranging from 120 to 130 GeV is performed to obtain the variations of the parameters of the Gaussian functions, described by polynomials in m_{H}, used in the signal model fit.

The final fit function for each category is obtained by summing the functions for all production modes normalised to the expected signal yields in that category. Figure 3 shows the signal model corresponding to $m_{\mathrm{H}} = 125\,\mathrm{GeV}$ for the best resolution category, which is the untagged events with the highest signal-to-background ratio and the highest diphoton BDT score, 'Untagged 0'. Also shown in the same figure is the signal model for the sum of all categories, with

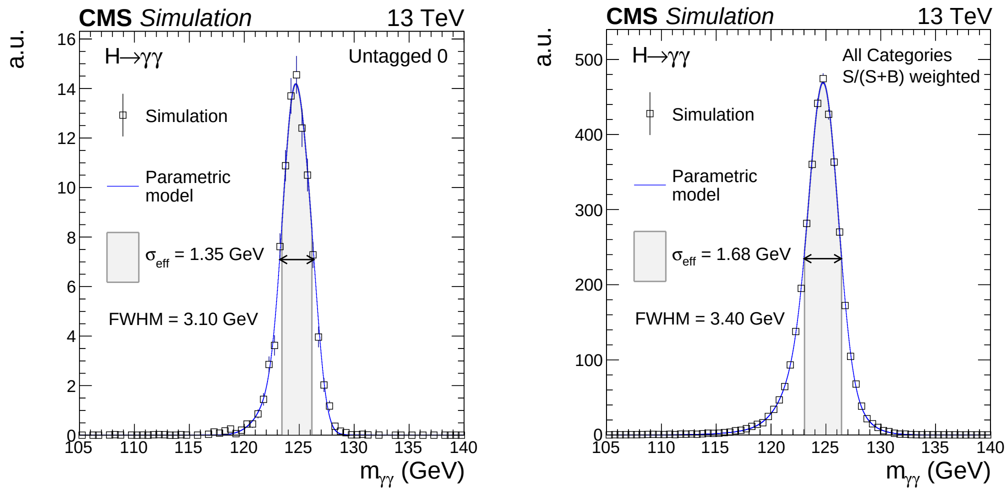

Figure 3: The signal shape models for the highest resolution analysis category (left), and the sum of all categories combined together after scaling each of them by the corresponding S/(S+B) ratio (right) for a simulated $H \to \gamma\gamma$ signal sample with $m_H = 125\,\text{GeV}$. The open squares represent weighted simulated events and the blue line represents the corresponding model. Also shown are the σ_{eff} value (half the width of the narrowest interval containing 68.3% of the invariant mass distribution) and the full width at half maximum (FWHM).

each category weighted by the corresponding S/(S+B) ratio, where S is the number of signal events, and B is the number of background events in a window around the m_H peak. In the figure the effective width (σ_{eff}), defined as half of the smallest interval that contains 68.3% of the invariant mass distribution, is given, as is the full width at half maximum (FWHM).

7.2 Background model

The model used to describe the background for each of the analysis categories is obtained from data using the discrete profiling method [19]. In this method, a large set of candidate function families is considered, including exponential functions, Bernstein polynomials, Laurent series, and power law functions. These are fit to the $m_{\gamma\gamma}$ distribution in the mass range of 100 to 180 GeV. For each family of functions, a Fisher test [20] is performed to determine the maximum order to be used in the fit, while the minimum order is determined by placing a requirement on the goodness of the fit to the data. The choice of the background function is treated as a discrete nuisance parameter in the fit to account for the uncertainty associated with the arbitrary choice of the function.

8 Systematic uncertainties

The systematic uncertainties are treated differently depending on their effect on the diphoton invariant mass distributions in the different signal categories. The systematic uncertainties in the photon energy scale and resolution modify the shape of the diphoton mass distribution in the signal model. Other systematic uncertainties, while not affecting the signal shape, affect the event yield. The sources of uncertainty included in previous CMS $H \to \gamma\gamma$ analyses are described in Ref. [9]. A more precise determination of the systematic uncertainties in the photon energy scale and resolution has been developed for the present analysis and is described here.

8.1 Uncertainties in the photon energy scale estimated with electrons

The following sources of systematic uncertainties in the photon energy scale were first estimated using electrons and propagated to the photons.

- *Electron energy scale and resolution*: The uncertainty in the electron energy scale and resolution corrections are derived using $Z \rightarrow ee$ events by varying the distribution of R_9, the electron selections used in the derivation of the corrections, and the transverse energy thresholds on the electron pairs used in the derivation of the corrections. This uncertainty is 0.05–0.1% for electrons in the EB, and 0.1–0.3% for electrons in the ECAL endcaps.
- *Residual p_T dependence of the energy scale correction*: Since the corrections for the residual differences between data and simulation were estimated with $Z \rightarrow ee$ events ($\langle p_T \rangle \approx 45\,\text{GeV}$), applying them to photons with $\langle p_T \rangle \approx 60\,\text{GeV}$ introduces an additional systematic error. The degree of nonclosure of the p_T-dependent electron energy scale corrections, as described in Section 5.1, is used as the estimate of this source of uncertainty, and is indicated by the band labelled as nonlinearity in Fig. 1. For electrons having $p_T < 80\,\text{GeV}$, corresponding to all analysis categories except the Untagged 0 category, this uncertainty is 0.075%. For electrons having p_T greater than 80 GeV, corresponding to the Untagged 0 category, the uncertainty is 0.15%. This uncertainty is applied conservatively on the global energy scale and is correlated among all photon candidates.

8.2 Uncertainties due to differences between electrons and photons

Additional systematic uncertainties due to the differences between the response of ECAL to electrons and photons were studied and assigned as follows:

- *Modelling of the material budget*: The uncertainty in the material budget between the interaction point and the ECAL, which affects electron and photon showers differently, was evaluated as described in Ref. [9], and is at most 0.24% of the photon energy scale.
- *Nonuniformity of the light collection*: The shower maximum for photons is deeper than that of electrons by approximately one radiation length, which is 0.89 cm in lead tungstate. Hence the differences in the light collection efficiency along the length of the ECAL crystals will introduce a difference in the ECAL response to electrons and photons. To account for this, an additional systematic uncertainty is assigned to the photon energy scale. Due to the increase in the radiation damage to the ECAL crystals in Run 2 compared to Run 1, the impact of the nonuniformity in light collection efficiency has become more important. Therefore, a special effort has been made to study this effect and to better estimate the associated systematic uncertainty in the photon energy scale. This is estimated using a light collection efficiency model derived from a detailed optical simulation [21] and validated with measurements made with irradiated crystals [22]. This model takes into account the nonuniformity of the collection of scintillation light due to radiation damage and the crystal geometry. This uncertainty has been evaluated as a function of p_T, supercluster $|\eta_{SC}|$, and R_9 using the radiation damage conditions experienced in the 2016 data taking period. The results are summarised in Fig. 4. The effect is less than 0.16% in the barrel and less than 0.45% in the endcap, and affects photons with $R_9 > 0.96$ the most. The uncertainty is assumed to be correlated among the different $|\eta|$ and R_9 bins but uncorrelated between the barrel and endcap regions due to the difference in the degree

of radiation damage and crystal size.

- *Mis-modelling of the input variables to the energy correction*: The uncertainty in the photon energy scale due to imperfect modelling of the shower shape in the simulation is found to be negligible (less than 10 MeV) as a result of the good agreement between data and simulation in the different input variables used in the photon energy regression correction.

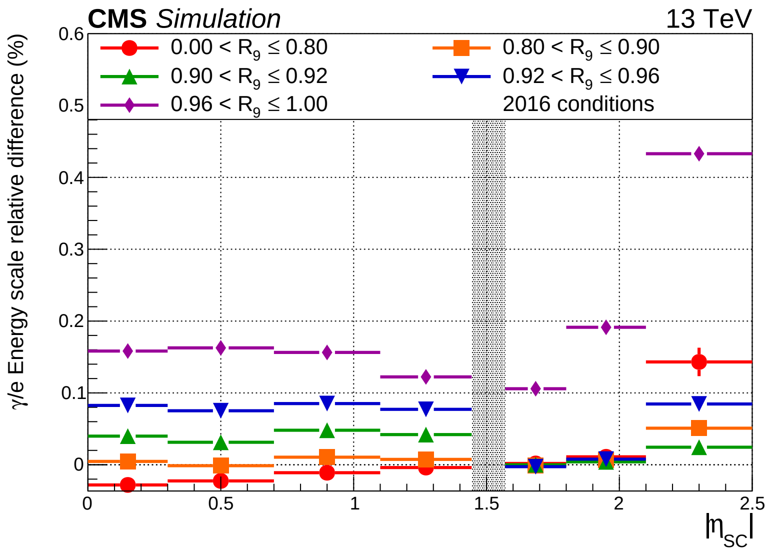

Figure 4: The systematic uncertainty due to the difference between the electron and photon energy scales from the radiation damage induced nonuniformity of light collection in ECAL crystals in different supercluster $|\eta_{SC}|$ and R_9 categories. The method used to evaluate this uncertainty is described in Section 8.2.

8.3 Impact of the sources of uncertainty

The contribution of each source of the photon energy scale systematic uncertainty to the total uncertainty in the m_H measurement was evaluated by performing a likelihood scan removing all but that source and subtracting the statistical uncertainty in quadrature. The results are summarised in Table 1. The leading sources of systematic uncertainty affecting m_H are the residual p_T dependence of the photon energy scale, nonuniformity of light collection, and the electron energy scale and resolution correction. The impact of all other sources of systematic uncertainty were found to be negligible.

Table 1: The observed impact of the different uncertainties on the measurement of m_H

Source	Contribution (GeV)
Electron energy scale and resolution corrections	0.10
Residual p_T dependence of the photon energy scale	0.11
Modelling of the material budget	0.03
Nonuniformity of the light collection	0.11
Total systematic uncertainty	0.18
Statistical uncertainty	0.18
Total uncertainty	0.26

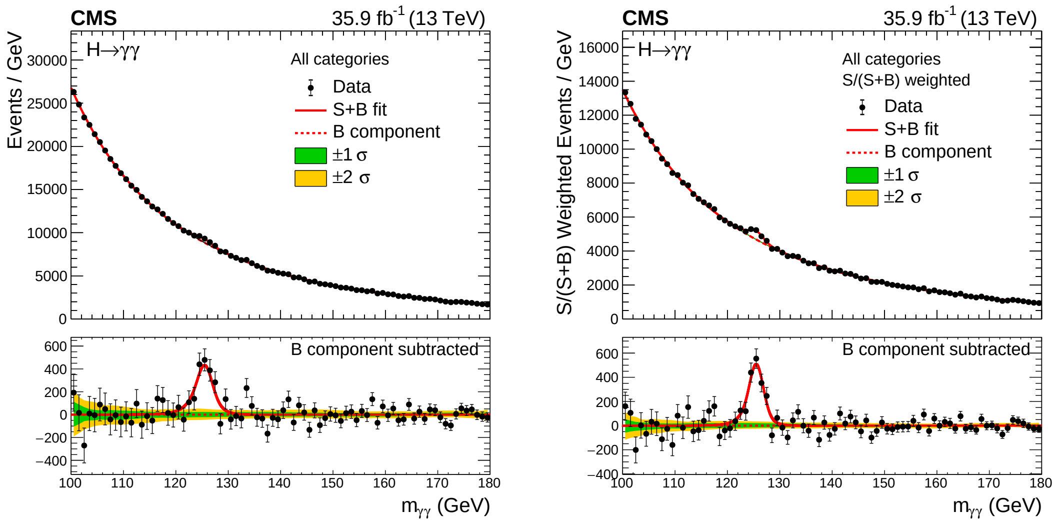

Figure 5: Data and signal-plus-background model fit for all categories summed (left) and where the categories are summed weighted by their corresponding sensitivities, given by S/(S+B) (right). The one (green) and two (yellow) standard deviation bands include the uncertainties in the background component of the fit. The lower panel in each plot shows the residuals after the background subtraction.

9 Results

To extract the measured value of m_{H} and its uncertainty, a binned maximum likelihood fit is performed simultaneously to the $m_{\gamma\gamma}$ distributions of the seven analysis categories described in Sec. 6, in the range $100 < m_{\gamma\gamma} < 180\,\mathrm{GeV}$. We use binned fits to reduce computation time and a bin size of 0.125 GeV, which is small compared to the diphoton mass resolution. The data and the signal-plus-background model fit for the sum of all analysis categories is shown in Fig. 5.

The expected number of signal events for each category is summarised in Fig. 6, where the contribution of each production mode to each analysis category is shown. The σ_{eff} and σ_{HM} are also listed; the latter is the FWHM, divided by 2.35.

In the likelihood scan of m_{H}, other parameters of the signal and background models are allowed to vary. Systematic uncertainties are included in the form of nuisance parameters, and the results are obtained using an asymptotic approach [23] with a test statistic based on the profile likelihood ratio [24]. In the fit to extract m_{H}, two independent signal strengths for the (ggH, $\mathrm{t\bar{t}H}$) $\to \gamma\gamma$ and (VBF, VH) $\to \gamma\gamma$ processes are free to vary. The best-fit mass of m_{H} is observed to be $m_{\mathrm{H}} = 125.78 \pm 0.18\,(\mathrm{stat}) \pm 0.18\,(\mathrm{syst})\,\mathrm{GeV}$, while it was expected to have a statistical uncertainty of $\pm 0.21\,\mathrm{GeV}$ and a systematic uncertainty of $\pm 0.18\,\mathrm{GeV}$. The signal strengths obtained were found to be compatible with the same from previous analysis in the diphoton decay channel [9]. The expected uncertainties in the measurement were obtained by generating an Asimov data set [24] from the expected signal from the standard model plus best-fit background model. The difference between the measured values of m_{H} in the $\mathrm{H} \to \gamma\gamma$ channel in the two LHC run periods, Run 1 [10] and 2016, is $\Delta m_{\mathrm{H}} = 1.12 \pm 0.43\,\mathrm{GeV}$. The compatibility of these two results is at the level of 2.6 standard deviations. A detailed set of cross-checks was performed to ensure that this shift is statistical.

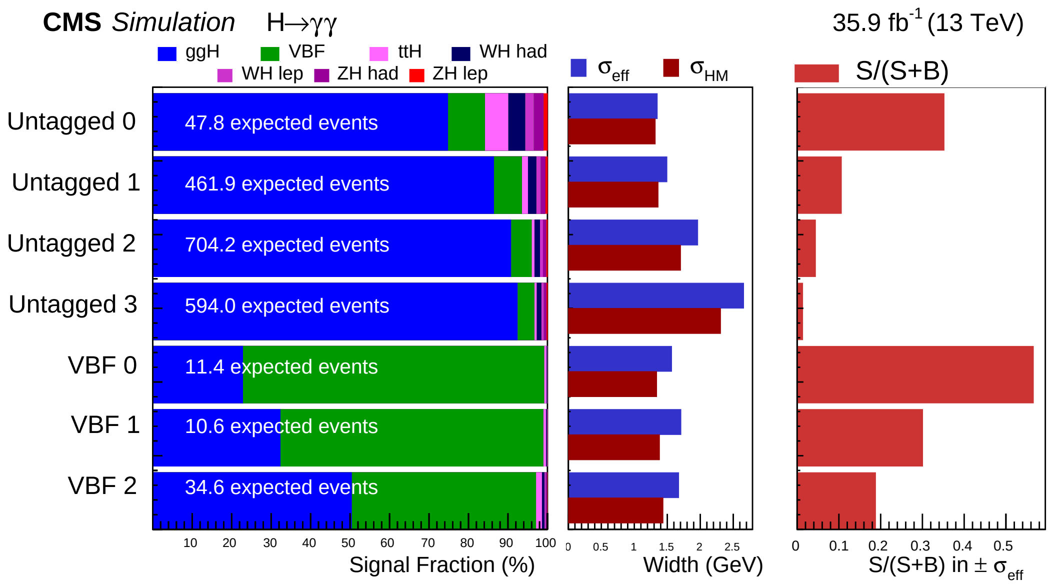

Figure 6: The expected number of signal events per category and the percentage breakdown per production mode. The σ_{eff} value (half the width of the narrowest interval containing 68.3% of the invariant mass distribution) is also shown as an estimate of the $m_{\gamma\gamma}$ resolution in that category and compared directly to the σ_{HM}. The ratio of the number of signal events (S) to the number of signal plus background events (S+B) is shown on the right-hand panel.

9.1 Combination with the H $\rightarrow$ ZZ $\rightarrow 4\ell$ mass measurement in the 2016 and Run 1 data sets

The results of this mass measurement were combined with a measurement of the same quantity in the H $\rightarrow$ ZZ $\rightarrow 4\ell$ decay channel with the 2016 data set reported by CMS in Ref. [5] using the same data set with a preliminary set of detector conditions.

In the combination a possible correlation may exist between electron and photon energy scales. In the H $\rightarrow \gamma\gamma$ decay channel, the largest contribution to the uncertainty on the photon energy scale is due to the difference in the calorimeter response to electrons and photons, which is only applied to the H $\rightarrow \gamma\gamma$ decay channel. Other differences between the two decay channels in the derivation of the energy scale corrections are the much finer binning in R_9 and their p_{T}-dependence in the H $\rightarrow \gamma\gamma$ decay channel. Additionally the average energy of the electrons in the H $\rightarrow$ ZZ $\rightarrow 4\ell$ decay channel is much lower than the most probable photon energy in the H $\rightarrow \gamma\gamma$ decay channel. Thus we treat the uncertainties, residual to the electron-photon difference, in the electron and photon energy scales to be uncorrelated between the two channels.

The combined value of m_{H} measured from the 2016 data set is observed to be $m_{\text{H}} = 125.46 \pm 0.13\,(\text{stat}) \pm 0.10\,(\text{syst})\,\text{GeV}$ with an expected statistical uncertainty of $\pm 0.16\,\text{GeV}$ and an expected systematic uncertainty of $\pm 0.10\,\text{GeV}$. Three independent signal strengths for the (ggH, $\text{t}\bar{\text{t}}$H) $\rightarrow \gamma\gamma$, (VBF, VH) $\rightarrow \gamma\gamma$ and pp $\rightarrow$ H $\rightarrow$ ZZ $\rightarrow 4\ell$ processes are free to vary in the fit to extract m_{H}, so that we are not completely dependent on the standard model for the production and decay ratios. This result is in good agreement with the ATLAS+CMS Run 1 measurement [4], $m_{\text{H}} = 125.09 \pm 0.24\,\text{GeV}$. A scan of the value of twice the negative logarithm of the likelihood ($-2\Delta \ln L$) as a function of m_{H} for the two individual decay channels, as well as their combination is shown in Fig. 7.

The same procedure was used to combine this result from the 2016 data set with the same measurement (H $\rightarrow \gamma\gamma$ and H $\rightarrow$ ZZ $\rightarrow 4\ell$) obtained from the Run 1 data [25]. The result

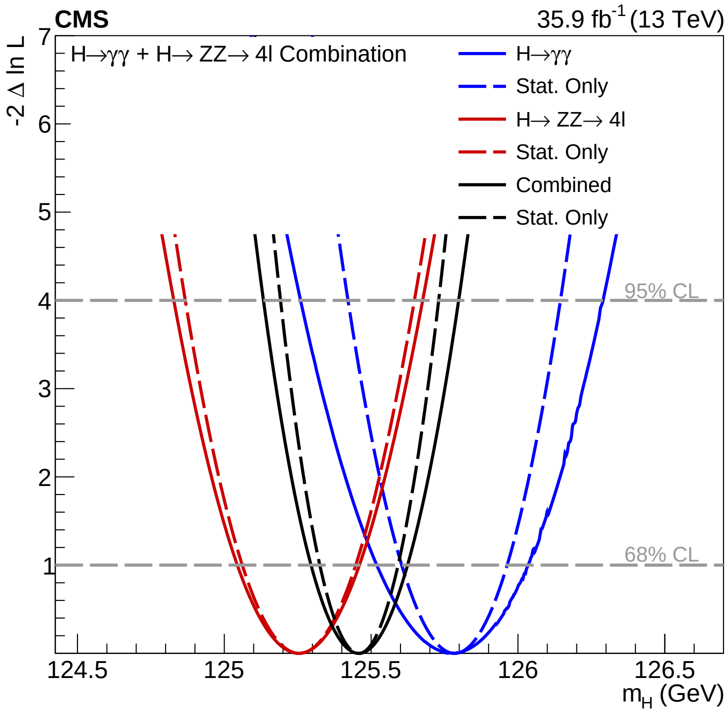

Figure 7: The likelihood scan of the measured Higgs boson mass in the $\mathrm{H} \to \gamma\gamma$ and $\mathrm{H} \to \mathrm{ZZ} \to 4\ell$ decay channels individually and for the combination with the 2016 data set. The solid lines are for the full likelihood scan including all systematic uncertainties, while the dashed lines denote the same with the statistical uncertainty only.

of combining the measurements from both data taking periods is $m_{\mathrm{H}} = 125.38 \pm 0.11\,(\mathrm{stat}) \pm 0.08\,(\mathrm{syst})\,\mathrm{GeV}$ with an expected statistical uncertainty of $\pm 0.13\,\mathrm{GeV}$ and an expected systematic uncertainty of $\pm 0.08\,\mathrm{GeV}$. Figure 8 shows the likelihood scans of the combined Higgs boson mass in the $\mathrm{H} \to \gamma\gamma$ and $\mathrm{H} \to \mathrm{ZZ} \to 4\ell$ decay channels with the Run 1 and 2016 data sets individually and the same combining the two data sets. A summary of the individual and combined measurements with the Run 1 and 2016 data sets is shown in Fig. 9.

10 Summary

In this Letter we describe a measurement of the Higgs boson mass in the diphoton decay channel with $35.9\,\mathrm{fb}^{-1}$ of data collected in 2016 at $\sqrt{s} = 13\,\mathrm{TeV}$ at the LHC. New analysis techniques have been introduced to improve the precision of the measurement and we have used a refined detector calibration. The technique that is new with respect to the previous analysis in the diphoton decay channel [9] is the introduction of residual energy corrections in much finer bins of η, p_{T} and the shower shape variable R_9 of the electrons from $\mathrm{Z} \to \mathrm{ee}$ decays, in which the electron showers are reconstructed as photons. We have also employed a new method to estimate the systematic uncertainty due to changes in the transparency of the crystals in the electromagnetic calorimeter with radiation damage. The measured value of the Higgs boson mass in the diphoton decay channel is found to be $m_{\mathrm{H}} = 125.78 \pm 0.26\,\mathrm{GeV}$. This measurement has been combined with a recent measurement by CMS of the same quantity in the $\mathrm{H} \to \mathrm{ZZ} \to 4\ell$ decay channel [5] to obtain a value of $m_{\mathrm{H}} = 125.46 \pm 0.16\,\mathrm{GeV}$. Furthermore, when the Run 2 result with the 2016 data set is combined with the same measurement performed in Run 1 at 7 and 8 TeV the value of the Higgs boson mass is found to be $m_{\mathrm{H}} = 125.38 \pm 0.14\,\mathrm{GeV}$. This is

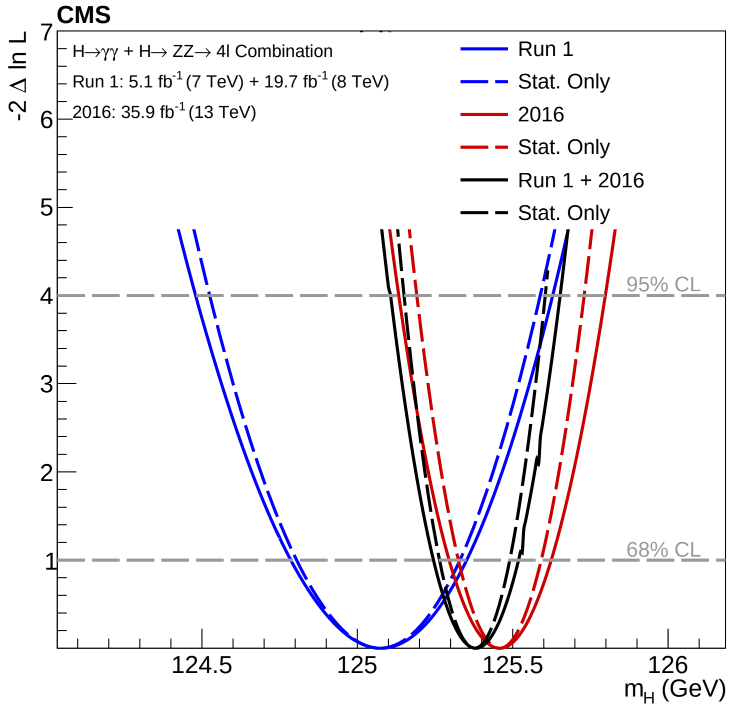

Figure 8: The likelihood scan of the combined Higgs boson mass in the $H \to \gamma\gamma$ and $H \to ZZ \to 4\ell$ decay channels with the Run 1 and 2016 data sets and the same combining the two data sets. The solid lines are for the full likelihood scan including all systematic uncertainties, while the dashed lines denote the same with the statistical uncertainty only.

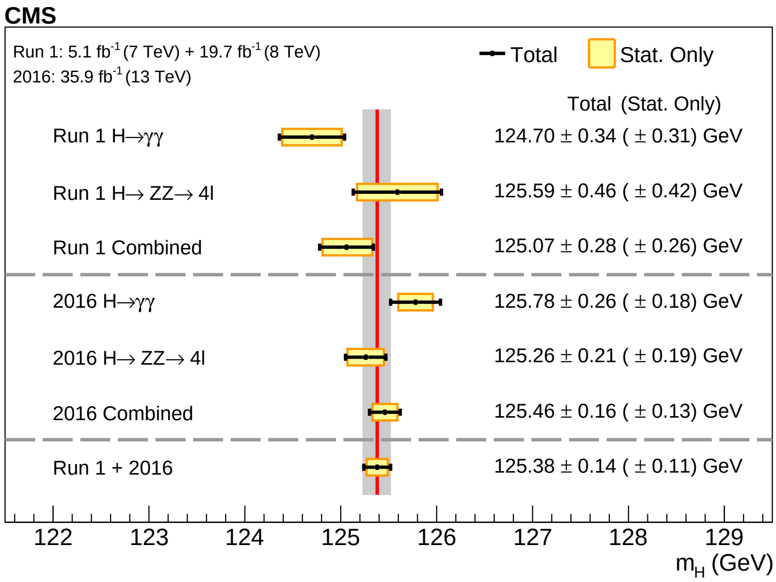

Figure 9: A summary of the measured Higgs boson mass in the $H \to \gamma\gamma$ and $H \to ZZ \to 4\ell$ decay channels, and for the combination of the two is presented here. The statistical (wider, yellow-shaded bands), and total (black error bars) uncertainties are indicated. The (red) vertical line and corresponding (grey) shaded column indicate the central value and the total uncertainty of the Run 1 + 2016 combined measurement, respectively.

currently the most precise measurement of the mass of the Higgs boson.

Acknowledgments

We congratulate our colleagues in the CERN accelerator departments for the excellent performance of the LHC and thank the technical and administrative staffs at CERN and at other CMS institutes for their contributions to the success of the CMS effort. In addition, we gratefully acknowledge the computing centres and personnel of the Worldwide LHC Computing Grid for delivering so effectively the computing infrastructure essential to our analyses. Finally, we acknowledge the enduring support for the construction and operation of the LHC and the CMS detector provided by the following funding agencies: BMBWF and FWF (Austria); FNRS and FWO (Belgium); CNPq, CAPES, FAPERJ, FAPERGS, and FAPESP (Brazil); MES (Bulgaria); CERN; CAS, MoST, and NSFC (China); COLCIENCIAS (Colombia); MSES and CSF (Croatia); RPF (Cyprus); SENESCYT (Ecuador); MoER, ERC IUT, PUT and ERDF (Estonia); Academy of Finland, MEC, and HIP (Finland); CEA and CNRS/IN2P3 (France); BMBF, DFG, and HGF (Germany); GSRT (Greece); NKFIA (Hungary); DAE and DST (India); IPM (Iran); SFI (Ireland); INFN (Italy); MSIP and NRF (Republic of Korea); MES (Latvia); LAS (Lithuania); MOE and UM (Malaysia); BUAP, CINVESTAV, CONACYT, LNS, SEP, and UASLP-FAI (Mexico); MOS (Montenegro); MBIE (New Zealand); PAEC (Pakistan); MSHE and NSC (Poland); FCT (Portugal); JINR (Dubna); MON, RosAtom, RAS, RFBR, and NRC KI (Russia); MESTD (Serbia); SEIDI, CPAN, PCTI, and FEDER (Spain); MOSTR (Sri Lanka); Swiss Funding Agencies (Switzerland); MST (Taipei); ThEPCenter, IPST, STAR, and NSTDA (Thailand); TUBITAK and TAEK (Turkey); NASU (Ukraine); STFC (United Kingdom); DOE and NSF (USA).

Individuals have received support from the Marie-Curie programme and the European Research Council and Horizon 2020 Grant, contract Nos. 675440, 752730, and 765710 (European Union); the Leventis Foundation; the A.P. Sloan Foundation; the Alexander von Humboldt Foundation; the Belgian Federal Science Policy Office; the Fonds pour la Formation à la Recherche dans l'Industrie et dans l'Agriculture (FRIA-Belgium); the Agentschap voor Innovatie door Wetenschap en Technologie (IWT-Belgium); the F.R.S.-FNRS and FWO (Belgium) under the "Excellence of Science – EOS" – be.h project n. 30820817; the Beijing Municipal Science & Technology Commission, No. Z191100007219010; the Ministry of Education, Youth and Sports (MEYS) of the Czech Republic; the Deutsche Forschungsgemeinschaft (DFG) under Germanys Excellence Strategy – EXC 2121 "Quantum Universe" – 390833306; the Lendület ("Momentum") Programme and the János Bolyai Research Scholarship of the Hungarian Academy of Sciences, the New National Excellence Program ÚNKP, the NKFIA research grants 123842, 123959, 124845, 124850, 125105, 128713, 128786, and 129058 (Hungary); the Council of Science and Industrial Research, India; the HOMING PLUS programme of the Foundation for Polish Science, cofinanced from European Union, Regional Development Fund, the Mobility Plus programme of the Ministry of Science and Higher Education, the National Science Center (Poland), contracts Harmonia 2014/14/M/ST2/00428, Opus 2014/13/B/ST2/02543, 2014/15/B/ST2/03998, and 2015/19/B/ST2/02861, Sonata-bis 2012/07/E/ST2/01406; the National Priorities Research Program by Qatar National Research Fund; the Ministry of Science and Education, grant no. 14.W03.31.0026 (Russia); the Programa Estatal de Fomento de la Investigación Científica y Técnica de Excelencia María de Maeztu, grant MDM-2015-0509 and the Programa Severo Ochoa del Principado de Asturias; the Thalis and Aristeia programmes cofinanced by EU-ESF and the Greek NSRF; the Rachadapisek Sompot Fund for Postdoctoral Fellowship, Chulalongkorn University and the Chulalongkorn Academic into Its 2nd Century Project Advancement Project (Thailand); the Kavli Foundation; the Nvidia Corporation; the SuperMicro Corporation; the Welch Foundation, contract C-1845; and the Weston Havens Foun-

dation (USA).

References

[1] ATLAS Collaboration, "Observation of a new particle in the search for the Standard Model Higgs boson with the ATLAS detector at the LHC", *Phys. Lett. B* **716** (2012) 1, doi:10.1016/j.physletb.2012.08.020, arXiv:1207.7214.

[2] CMS Collaboration, "Observation of a new boson at a mass of 125 GeV with the CMS experiment at the LHC", *Phys. Lett. B* **716** (2012) 30, doi:10.1016/j.physletb.2012.08.021, arXiv:1207.7235.

[3] CMS Collaboration, "Observation of a new boson with mass near 125 GeV in pp Collisions at $\sqrt{s}$ = 7 and 8 TeV", *JHEP* **06** (2013) 081, doi:10.1007/JHEP06(2013)081, arXiv:1303.4571.

[4] ATLAS and CMS Collaborations, "Combined measurement of the Higgs boson mass in pp collisions at $\sqrt{s} = 7$ and 8 TeV with the ATLAS and CMS experiments", *Phys. Rev. Lett.* **114** (2015) 191803, doi:10.1103/PhysRevLett.114.191803, arXiv:1503.07589.

[5] CMS Collaboration, "Measurements of properties of the Higgs boson decaying into the four-lepton final state in pp collisions at $\sqrt{s} = 13$ TeV", *JHEP* **11** (2017) 047, doi:10.1007/JHEP11(2017)047, arXiv:1706.09936.

[6] ATLAS Collaboration, "Measurement of the Higgs boson mass in the $H \to ZZ^* \to 4\ell$ and $H \to \gamma\gamma$ channels with $\sqrt{s} = 13$ TeV pp collisions using the ATLAS detector", *Phys. Lett. B* **784** (2018) 345, doi:10.1016/j.physletb.2018.07.050, arXiv:1806.00242.

[7] CMS Collaboration, "The CMS trigger system", *JINST* **12** (2017) P01020, doi:10.1088/1748-0221/12/01/P01020, arXiv:1609.02366.

[8] CMS Collaboration, "The CMS experiment at the CERN LHC", *JINST* **3** (2008) S08004, doi:10.1088/1748-0221/3/08/S08004.

[9] CMS Collaboration, "Measurements of Higgs boson properties in the diphoton decay channel in proton-proton collisions at $\sqrt{s} = 13$ TeV", *JHEP* **11** (2018) 185, doi:10.1007/JHEP11(2018)185, arXiv:1804.02716.

[10] CMS Collaboration, "Observation of the diphoton decay of the Higgs boson and measurement of its properties", *Eur. Phys. J. C* **74** (2014) 3076, doi:10.1140/epjc/s10052-014-3076-z, arXiv:1407.0558.

[11] GEANT4 Collaboration, "GEANT4—a simulation toolkit", *Nucl. Instrum. Meth. A* **506** (2003) 250, doi:10.1016/S0168-9002(03)01368-8.

[12] J. Alwall et al., "The automated computation of tree-level and next-to-leading order differential cross sections, and their matching to parton shower simulations", *JHEP* **07** (2014) 079, doi:10.1007/JHEP07(2014)079, arXiv:1405.0301.

[13] T. Sjöstrand, S. Mrenna, and P. Skands, "A brief introduction to PYTHIA 8.1", *Comput. Phys. Commun.* **178** (2007) 852, doi:10.1016/j.cpc.2008.01.036, arXiv:0710.3820.

[14] CMS Collaboration, "Event generator tunes obtained from underlying event and multiparton scattering measurements", *Eur. Phys. J. C* **76** (2016) 155, doi:10.1140/epjc/s10052-016-3988-x, arXiv:1512.00815.

[15] Sherpa Collaboration, "Event Generation with Sherpa 2.2", *SciPost Phys.* **7** (2019) 034, doi:10.21468/SciPostPhys.7.3.034, arXiv:1905.09127.

[16] J. Alwall et al., "MadGraph 5: going beyond", *JHEP* **06** (2011) 128, doi:10.1007/JHEP06(2011)128, arXiv:1106.0522.

[17] CMS Collaboration, "Energy calibration and resolution of the CMS electromagnetic calorimeter in pp collisions at $\sqrt{s} = 7$ TeV", *JINST* **8** (2013) P09009, doi:10.1088/1748-0221/8/09/P09009, arXiv:1306.2016.

[18] CMS Collaboration, "Performance of photon reconstruction and identification with the CMS detector in proton-proton Collisions at $\sqrt{s}$ = 8 TeV", *JINST* **10** (2015) P08010, doi:10.1088/1748-0221/10/08/P08010, arXiv:1502.02702.

[19] P. D. Dauncey, M. Kenzie, N. Wardle, and G. J. Davies, "Handling uncertainties in background shapes: the discrete profiling method", *JINST* **10** (2015) P04015, doi:10.1088/1748-0221/10/04/P04015, arXiv:1408.6865.

[20] R. A. Fisher, "On the interpretation of χ^2 from contingency tables, and the calculation of P", *J. Roy. Statis. Soc.* **85** (1922) 87, doi:10.2307/2340521.

[21] F. Gentit, "Litrani: a general purpose Monte-Carlo program simulating light propagation in isotropic or anisotropic media", *Nucl. Inst. Meth. A* **486** (2002) 35, doi:10.1016/S0168-9002(02)00671-X.

[22] T. Adams et al., "Beam test evaluation of electromagnetic calorimeter modules made from proton-damaged $PbWO_4$ crystals", *JINST* **11** (2016) P04012, doi:10.1088/1748-0221/11/04/p04012.

[23] ATLAS and CMS Collaborations, "Procedure for the LHC Higgs boson search combination in Summer 2011", Technical Report CMS-NOTE-2011-005. ATL-PHYS-PUB-2011-11, 2011.

[24] G. Cowan, K. Cranmer, E. Gross, and O. Vitells, "Asymptotic formulae for likelihood-based tests of new physics", *Eur. Phys. J. C* **71** (2011) 1554, doi:10.1140/epjc/s10052-011-1554-0, arXiv:1007.1727. [Erratum: doi:10.1140/epjc/s10052-013-2501-z].

[25] CMS Collaboration, "Precise determination of the mass of the Higgs boson and tests of compatibility of its couplings with the standard model predictions using proton collisions at 7 and 8 TeV", *Eur. Phys. J. C* **75** (2015) 212, doi:10.1140/epjc/s10052-015-3351-7, arXiv:1412.8662.

A The CMS Collaboration

Yerevan Physics Institute, Yerevan, Armenia
A.M. Sirunyan[†], A. Tumasyan

Institut für Hochenergiephysik, Wien, Austria
W. Adam, F. Ambrogi, T. Bergauer, M. Dragicevic, J. Erö, A. Escalante Del Valle, M. Flechl, R. Frühwirth[1], M. Jeitler[1], N. Krammer, I. Krätschmer, D. Liko, T. Madlener, I. Mikulec, N. Rad, J. Schieck[1], R. Schöfbeck, M. Spanring, W. Waltenberger, C.-E. Wulz[1], M. Zarucki

Institute for Nuclear Problems, Minsk, Belarus
V. Drugakov, V. Mossolov, J. Suarez Gonzalez

Universiteit Antwerpen, Antwerpen, Belgium
M.R. Darwish, E.A. De Wolf, D. Di Croce, X. Janssen, A. Lelek, M. Pieters, H. Rejeb Sfar, H. Van Haevermaet, P. Van Mechelen, S. Van Putte, N. Van Remortel

Vrije Universiteit Brussel, Brussel, Belgium
F. Blekman, E.S. Bols, S.S. Chhibra, J. D'Hondt, J. De Clercq, D. Lontkovskyi, S. Lowette, I. Marchesini, S. Moortgat, Q. Python, S. Tavernier, W. Van Doninck, P. Van Mulders

Université Libre de Bruxelles, Bruxelles, Belgium
D. Beghin, B. Bilin, B. Clerbaux, G. De Lentdecker, H. Delannoy, B. Dorney, L. Favart, A. Grebenyuk, A.K. Kalsi, L. Moureaux, A. Popov, N. Postiau, E. Starling, L. Thomas, C. Vander Velde, P. Vanlaer, D. Vannerom

Ghent University, Ghent, Belgium
T. Cornelis, D. Dobur, I. Khvastunov[2], M. Niedziela, C. Roskas, K. Skovpen, M. Tytgat, W. Verbeke, B. Vermassen, M. Vit

Université Catholique de Louvain, Louvain-la-Neuve, Belgium
O. Bondu, G. Bruno, C. Caputo, P. David, C. Delaere, M. Delcourt, A. Giammanco, V. Lemaitre, J. Prisciandaro, A. Saggio, M. Vidal Marono, P. Vischia, J. Zobec

Centro Brasileiro de Pesquisas Fisicas, Rio de Janeiro, Brazil
G.A. Alves, G. Correia Silva, C. Hensel, A. Moraes

Universidade do Estado do Rio de Janeiro, Rio de Janeiro, Brazil
E. Belchior Batista Das Chagas, W. Carvalho, J. Chinellato[3], E. Coelho, E.M. Da Costa, G.G. Da Silveira[4], D. De Jesus Damiao, C. De Oliveira Martins, S. Fonseca De Souza, L.M. Huertas Guativa, H. Malbouisson, J. Martins[5], D. Matos Figueiredo, M. Medina Jaime[6], M. Melo De Almeida, C. Mora Herrera, L. Mundim, H. Nogima, W.L. Prado Da Silva, P. Rebello Teles, L.J. Sanchez Rosas, A. Santoro, A. Sznajder, M. Thiel, E.J. Tonelli Manganote[3], F. Torres Da Silva De Araujo, A. Vilela Pereira

Universidade Estadual Paulista [a], Universidade Federal do ABC [b], São Paulo, Brazil
C.A. Bernardes[a], L. Calligaris[a], T.R. Fernandez Perez Tomei[a], E.M. Gregores[b], D.S. Lemos, P.G. Mercadante[b], S.F. Novaes[a], SandraS. Padula[a]

Institute for Nuclear Research and Nuclear Energy, Bulgarian Academy of Sciences, Sofia, Bulgaria
A. Aleksandrov, G. Antchev, R. Hadjiiska, P. Iaydjiev, M. Misheva, M. Rodozov, M. Shopova, G. Sultanov

University of Sofia, Sofia, Bulgaria
M. Bonchev, A. Dimitrov, T. Ivanov, L. Litov, B. Pavlov, P. Petkov, A. Petrov

Beihang University, Beijing, China
W. Fang[7], X. Gao[7], L. Yuan

Department of Physics, Tsinghua University, Beijing, China
M. Ahmad, Z. Hu, Y. Wang

Institute of High Energy Physics, Beijing, China
G.M. Chen[8], H.S. Chen[8], M. Chen, C.H. Jiang, D. Leggat, H. Liao, Z. Liu, A. Spiezia, J. Tao, E. Yazgan, H. Zhang, S. Zhang[8], J. Zhao

State Key Laboratory of Nuclear Physics and Technology, Peking University, Beijing, China
A. Agapitos, Y. Ban, G. Chen, A. Levin, J. Li, L. Li, Q. Li, Y. Mao, S.J. Qian, D. Wang, Q. Wang

Zhejiang University, Hangzhou, China
M. Xiao

Universidad de Los Andes, Bogota, Colombia
C. Avila, A. Cabrera, C. Florez, C.F. González Hernández, M.A. Segura Delgado

Universidad de Antioquia, Medellin, Colombia
J. Mejia Guisao, J.D. Ruiz Alvarez, C.A. Salazar González, N. Vanegas Arbelaez

University of Split, Faculty of Electrical Engineering, Mechanical Engineering and Naval Architecture, Split, Croatia
D. Giljanović, N. Godinovic, D. Lelas, I. Puljak, T. Sculac

University of Split, Faculty of Science, Split, Croatia
Z. Antunovic, M. Kovac

Institute Rudjer Boskovic, Zagreb, Croatia
V. Brigljevic, D. Ferencek, K. Kadija, B. Mesic, M. Roguljic, A. Starodumov[9], T. Susa

University of Cyprus, Nicosia, Cyprus
M.W. Ather, A. Attikis, E. Erodotou, A. Ioannou, M. Kolosova, S. Konstantinou, G. Mavromanolakis, J. Mousa, C. Nicolaou, F. Ptochos, P.A. Razis, H. Rykaczewski, H. Saka, D. Tsiakkouri

Charles University, Prague, Czech Republic
M. Finger[10], M. Finger Jr.[10], A. Kveton, J. Tomsa

Escuela Politecnica Nacional, Quito, Ecuador
E. Ayala

Universidad San Francisco de Quito, Quito, Ecuador
E. Carrera Jarrin

Academy of Scientific Research and Technology of the Arab Republic of Egypt, Egyptian Network of High Energy Physics, Cairo, Egypt
H. Abdalla[11], S. Elgammal[12]

National Institute of Chemical Physics and Biophysics, Tallinn, Estonia
S. Bhowmik, A. Carvalho Antunes De Oliveira, R.K. Dewanjee, K. Ehataht, M. Kadastik, M. Raidal, C. Veelken

Department of Physics, University of Helsinki, Helsinki, Finland
P. Eerola, L. Forthomme, H. Kirschenmann, K. Osterberg, M. Voutilainen

Helsinki Institute of Physics, Helsinki, Finland
F. Garcia, J. Havukainen, J.K. Heikkilä, V. Karimäki, M.S. Kim, R. Kinnunen, T. Lampén, K. Lassila-Perini, S. Laurila, S. Lehti, T. Lindén, H. Siikonen, E. Tuominen, J. Tuominiemi

Lappeenranta University of Technology, Lappeenranta, Finland
P. Luukka, T. Tuuva

IRFU, CEA, Université Paris-Saclay, Gif-sur-Yvette, France
M. Besancon, F. Couderc, M. Dejardin, D. Denegri, B. Fabbro, J.L. Faure, F. Ferri, S. Ganjour, A. Givernaud, P. Gras, G. Hamel de Monchenault, P. Jarry, C. Leloup, B. Lenzi, E. Locci, J. Malcles, J. Rander, A. Rosowsky, M.Ö. Sahin, A. Savoy-Navarro[13], M. Titov, G.B. Yu

Laboratoire Leprince-Ringuet, CNRS/IN2P3, Ecole Polytechnique, Institut Polytechnique de Paris
S. Ahuja, C. Amendola, F. Beaudette, P. Busson, C. Charlot, B. Diab, G. Falmagne, R. Granier de Cassagnac, I. Kucher, A. Lobanov, C. Martin Perez, M. Nguyen, C. Ochando, P. Paganini, J. Rembser, R. Salerno, J.B. Sauvan, Y. Sirois, A. Zabi, A. Zghiche

Université de Strasbourg, CNRS, IPHC UMR 7178, Strasbourg, France
J.-L. Agram[14], J. Andrea, D. Bloch, G. Bourgatte, J.-M. Brom, E.C. Chabert, C. Collard, E. Conte[14], J.-C. Fontaine[14], D. Gelé, U. Goerlach, C. Grimault, M. Jansová, A.-C. Le Bihan, N. Tonon, P. Van Hove

Centre de Calcul de l'Institut National de Physique Nucleaire et de Physique des Particules, CNRS/IN2P3, Villeurbanne, France
S. Gadrat

Université de Lyon, Université Claude Bernard Lyon 1, CNRS-IN2P3, Institut de Physique Nucléaire de Lyon, Villeurbanne, France
S. Beauceron, C. Bernet, G. Boudoul, C. Camen, A. Carle, N. Chanon, R. Chierici, D. Contardo, P. Depasse, H. El Mamouni, J. Fay, S. Gascon, M. Gouzevitch, B. Ille, Sa. Jain, I.B. Laktineh, H. Lattaud, A. Lesauvage, M. Lethuillier, L. Mirabito, S. Perries, V. Sordini, L. Torterotot, G. Touquet, M. Vander Donckt, S. Viret

Georgian Technical University, Tbilisi, Georgia
A. Khvedelidze[10]

Tbilisi State University, Tbilisi, Georgia
Z. Tsamalaidze[10]

RWTH Aachen University, I. Physikalisches Institut, Aachen, Germany
C. Autermann, L. Feld, K. Klein, M. Lipinski, D. Meuser, A. Pauls, M. Preuten, M.P. Rauch, J. Schulz, M. Teroerde

RWTH Aachen University, III. Physikalisches Institut A, Aachen, Germany
M. Erdmann, B. Fischer, S. Ghosh, T. Hebbeker, K. Hoepfner, H. Keller, L. Mastrolorenzo, M. Merschmeyer, A. Meyer, P. Millet, G. Mocellin, S. Mondal, S. Mukherjee, D. Noll, A. Novak, T. Pook, A. Pozdnyakov, T. Quast, M. Radziej, Y. Rath, H. Reithler, J. Roemer, A. Schmidt, S.C. Schuler, A. Sharma, S. Wiedenbeck, S. Zaleski

RWTH Aachen University, III. Physikalisches Institut B, Aachen, Germany
G. Flügge, W. Haj Ahmad[15], O. Hlushchenko, T. Kress, T. Müller, A. Nowack, C. Pistone, O. Pooth, D. Roy, H. Sert, A. Stahl[16]

Deutsches Elektronen-Synchrotron, Hamburg, Germany
M. Aldaya Martin, P. Asmuss, I. Babounikau, H. Bakhshiansohi, K. Beernaert, O. Behnke, A. Bermúdez Martínez, A.A. Bin Anuar, K. Borras[17], V. Botta, A. Campbell, A. Cardini, P. Connor, S. Consuegra Rodríguez, C. Contreras-Campana, V. Danilov, A. De Wit, M.M. Defranchis, C. Diez Pardos, D. Domínguez Damiani, G. Eckerlin, D. Eckstein, T. Eichhorn, A. Elwood, E. Eren, E. Gallo[18], A. Geiser, A. Grohsjean, M. Guthoff, M. Haranko, A. Harb, A. Jafari, N.Z. Jomhari, H. Jung, A. Kasem[17], M. Kasemann, H. Kaveh, J. Keaveney, C. Kleinwort, J. Knolle, D. Krücker, W. Lange, T. Lenz, J. Lidrych, K. Lipka, W. Lohmann[19], R. Mankel, I.-A. Melzer-Pellmann, A.B. Meyer, M. Meyer, M. Missiroli, J. Mnich, A. Mussgiller, V. Myronenko, D. Pérez Adán, S.K. Pflitsch, D. Pitzl, A. Raspereza, A. Saibel, M. Savitskyi, V. Scheurer, P. Schütze, C. Schwanenberger, R. Shevchenko, A. Singh, R.E. Sosa Ricardo, H. Tholen, O. Turkot, A. Vagnerini, M. Van De Klundert, R. Walsh, Y. Wen, K. Wichmann, C. Wissing, O. Zenaiev, R. Zlebcik

University of Hamburg, Hamburg, Germany
R. Aggleton, S. Bein, L. Benato, A. Benecke, T. Dreyer, A. Ebrahimi, F. Feindt, A. Fröhlich, C. Garbers, E. Garutti, D. Gonzalez, P. Gunnellini, J. Haller, A. Hinzmann, A. Karavdina, G. Kasieczka, R. Klanner, R. Kogler, N. Kovalchuk, S. Kurz, V. Kutzner, J. Lange, T. Lange, A. Malara, J. Multhaup, C.E.N. Niemeyer, A. Reimers, O. Rieger, P. Schleper, S. Schumann, J. Schwandt, J. Sonneveld, H. Stadie, G. Steinbrück, B. Vormwald, I. Zoi

Karlsruher Institut fuer Technologie, Karlsruhe, Germany
M. Akbiyik, M. Baselga, S. Baur, T. Berger, E. Butz, R. Caspart, T. Chwalek, W. De Boer, A. Dierlamm, K. El Morabit, N. Faltermann, M. Giffels, A. Gottmann, F. Hartmann[16], C. Heidecker, U. Husemann, S. Kudella, S. Maier, S. Mitra, M.U. Mozer, D. Müller, Th. Müller, M. Musich, A. Nürnberg, G. Quast, K. Rabbertz, D. Schäfer, M. Schröder, I. Shvetsov, H.J. Simonis, R. Ulrich, M. Wassmer, M. Weber, C. Wöhrmann, R. Wolf, S. Wozniewski

Institute of Nuclear and Particle Physics (INPP), NCSR Demokritos, Aghia Paraskevi, Greece
G. Anagnostou, P. Asenov, G. Daskalakis, T. Geralis, A. Kyriakis, D. Loukas, G. Paspalaki

National and Kapodistrian University of Athens, Athens, Greece
M. Diamantopoulou, G. Karathanasis, P. Kontaxakis, A. Manousakis-katsikakis, A. Panagiotou, I. Papavergou, N. Saoulidou, A. Stakia, K. Theofilatos, K. Vellidis, E. Vourliotis

National Technical University of Athens, Athens, Greece
G. Bakas, K. Kousouris, I. Papakrivopoulos, G. Tsipolitis, A. Zacharopoulou

University of Ioánnina, Ioánnina, Greece
I. Evangelou, C. Foudas, P. Gianneios, P. Katsoulis, P. Kokkas, S. Mallios, K. Manitara, N. Manthos, I. Papadopoulos, J. Strologas, F.A. Triantis, D. Tsitsonis

MTA-ELTE Lendület CMS Particle and Nuclear Physics Group, Eötvös Loránd University, Budapest, Hungary
M. Bartók[20], R. Chudasama, M. Csanad, P. Major, K. Mandal, A. Mehta, G. Pasztor, O. Surányi, G.I. Veres

Wigner Research Centre for Physics, Budapest, Hungary
G. Bencze, C. Hajdu, D. Horvath[21], F. Sikler, V. Veszpremi, G. Vesztergombi[†]

Institute of Nuclear Research ATOMKI, Debrecen, Hungary
N. Beni, S. Czellar, J. Karancsi[20], J. Molnar, Z. Szillasi

Institute of Physics, University of Debrecen, Debrecen, Hungary
P. Raics, D. Teyssier, Z.L. Trocsanyi, B. Ujvari

Eszterhazy Karoly University, Karoly Robert Campus, Gyongyos, Hungary
T. Csorgo, W.J. Metzger, F. Nemes, T. Novak

Indian Institute of Science (IISc), Bangalore, India
S. Choudhury, J.R. Komaragiri, P.C. Tiwari

National Institute of Science Education and Research, HBNI, Bhubaneswar, India
S. Bahinipati[23], C. Kar, G. Kole, P. Mal, V.K. Muraleedharan Nair Bindhu, A. Nayak[24], D.K. Sahoo[23], S.K. Swain

Panjab University, Chandigarh, India
S. Bansal, S.B. Beri, V. Bhatnagar, S. Chauhan, N. Dhingra[25], R. Gupta, A. Kaur, M. Kaur, S. Kaur, P. Kumari, M. Lohan, M. Meena, K. Sandeep, S. Sharma, J.B. Singh, A.K. Virdi

University of Delhi, Delhi, India
A. Bhardwaj, B.C. Choudhary, R.B. Garg, M. Gola, S. Keshri, Ashok Kumar, M. Naimuddin, P. Priyanka, K. Ranjan, Aashaq Shah, R. Sharma

Saha Institute of Nuclear Physics, HBNI, Kolkata, India
R. Bhardwaj[26], M. Bharti[26], R. Bhattacharya, S. Bhattacharya, U. Bhawandeep[26], D. Bhowmik, S. Dutta, S. Ghosh, B. Gomber[27], M. Maity[28], K. Mondal, S. Nandan, A. Purohit, P.K. Rout, G. Saha, S. Sarkar, T. Sarkar[28], M. Sharan, B. Singh[26], S. Thakur[26]

Indian Institute of Technology Madras, Madras, India
P.K. Behera, S.C. Behera, P. Kalbhor, A. Muhammad, P.R. Pujahari, A. Sharma, A.K. Sikdar

Bhabha Atomic Research Centre, Mumbai, India
D. Dutta, V. Jha, D.K. Mishra, P.K. Netrakanti, L.M. Pant, P. Shukla

Tata Institute of Fundamental Research-A, Mumbai, India
T. Aziz, M.A. Bhat, S. Dugad, G.B. Mohanty, N. Sur, RavindraKumar Verma

Tata Institute of Fundamental Research-B, Mumbai, India
S. Banerjee, S. Bhattacharya, S. Chatterjee, P. Das, M. Guchait, S. Karmakar, S. Kumar, G. Majumder, K. Mazumdar, N. Sahoo, S. Sawant

Indian Institute of Science Education and Research (IISER), Pune, India
S. Dube, B. Kansal, A. Kapoor, K. Kothekar, S. Pandey, A. Rane, A. Rastogi, S. Sharma

Institute for Research in Fundamental Sciences (IPM), Tehran, Iran
S. Chenarani, S.M. Etesami, M. Khakzad, M. Mohammadi Najafabadi, M. Naseri, F. Rezaei Hosseinabadi

University College Dublin, Dublin, Ireland
M. Felcini, M. Grunewald

INFN Sezione di Bari [a], Università di Bari [b], Politecnico di Bari [c], Bari, Italy
M. Abbrescia[a,b], R. Aly[a,b,29], C. Calabria[a,b], A. Colaleo[a], D. Creanza[a,c], L. Cristella[a,b], N. De Filippis[a,c], M. De Palma[a,b], A. Di Florio[a,b], W. Elmetenawee[a,b], L. Fiore[a], A. Gelmi[a,b], G. Iaselli[a,c], M. Ince[a,b], S. Lezki[a,b], G. Maggi[a,c], M. Maggi[a], J.A. Merlin[a], G. Miniello[a,b], S. My[a,b], S. Nuzzo[a,b], A. Pompili[a,b], G. Pugliese[a,c], R. Radogna[a], A. Ranieri[a], G. Selvaggi[a,b], L. Silvestris[a], F.M. Simone[a,b], R. Venditti[a], P. Verwilligen[a]

INFN Sezione di Bologna [a], Università di Bologna [b], Bologna, Italy
G. Abbiendi[a], C. Battilana[a,b], D. Bonacorsi[a,b], L. Borgonovi[a,b], S. Braibant-Giacomelli[a,b], R. Campanini[a,b], P. Capiluppi[a,b], A. Castro[a,b], F.R. Cavallo[a], C. Ciocca[a], G. Codispoti[a,b], M. Cuffiani[a,b], G.M. Dallavalle[a], F. Fabbri[a], A. Fanfani[a,b], E. Fontanesi[a,b], P. Giacomelli[a], C. Grandi[a], L. Guiducci[a,b], F. Iemmi[a,b], S. Lo Meo[a,30], S. Marcellini[a], G. Masetti[a], F.L. Navarria[a,b], A. Perrotta[a], F. Primavera[a,b], A.M. Rossi[a,b], T. Rovelli[a,b], G.P. Siroli[a,b], N. Tosi[a]

INFN Sezione di Catania [a], Università di Catania [b], Catania, Italy
S. Albergo[a,b,31], S. Costa[a,b], A. Di Mattia[a], R. Potenza[a,b], A. Tricomi[a,b,31], C. Tuve[a,b]

INFN Sezione di Firenze [a], Università di Firenze [b], Firenze, Italy
G. Barbagli[a], A. Cassese, R. Ceccarelli, V. Ciulli[a,b], C. Civinini[a], R. D'Alessandro[a,b], F. Fiori[a,c], E. Focardi[a,b], G. Latino[a,b], P. Lenzi[a,b], M. Meschini[a], S. Paoletti[a], G. Sguazzoni[a], L. Viliani[a]

INFN Laboratori Nazionali di Frascati, Frascati, Italy
L. Benussi, S. Bianco, D. Piccolo

INFN Sezione di Genova [a], Università di Genova [b], Genova, Italy
M. Bozzo[a,b], F. Ferro[a], R. Mulargia[a,b], E. Robutti[a], S. Tosi[a,b]

INFN Sezione di Milano-Bicocca [a], Università di Milano-Bicocca [b], Milano, Italy
A. Benaglia[a], A. Beschi[a,b], F. Brivio[a,b], V. Ciriolo[a,b,16], M.E. Dinardo[a,b], P. Dini[a], S. Gennai[a], A. Ghezzi[a,b], P. Govoni[a,b], L. Guzzi[a,b], M. Malberti[a], S. Malvezzi[a], D. Menasce[a], F. Monti[a,b], L. Moroni[a], M. Paganoni[a,b], D. Pedrini[a], S. Ragazzi[a,b], T. Tabarelli de Fatis[a,b], D. Valsecchi[a,b], D. Zuolo[a,b]

INFN Sezione di Napoli [a], Università di Napoli 'Federico II' [b], Napoli, Italy, Università della Basilicata [c], Potenza, Italy, Università G. Marconi [d], Roma, Italy
S. Buontempo[a], N. Cavallo[a,c], A. De Iorio[a,b], A. Di Crescenzo[a,b], F. Fabozzi[a,c], F. Fienga[a], G. Galati[a], A.O.M. Iorio[a,b], L. Layer[a,b], L. Lista[a,b], S. Meola[a,d,16], P. Paolucci[a,16], B. Rossi[a], C. Sciacca[a,b], E. Voevodina[a,b]

INFN Sezione di Padova [a], Università di Padova [b], Padova, Italy, Università di Trento [c], Trento, Italy
P. Azzi[a], N. Bacchetta[a], D. Bisello[a,b], A. Boletti[a,b], A. Bragagnolo[a,b], R. Carlin[a,b], P. Checchia[a], P. De Castro Manzano[a], T. Dorigo[a], U. Dosselli[a], F. Gasparini[a,b], U. Gasparini[a,b], A. Gozzelino[a], S.Y. Hoh[a,b], M. Margoni[a,b], A.T. Meneguzzo[a,b], J. Pazzini[a,b], M. Presilla[b], P. Ronchese[a,b], R. Rossin[a,b], F. Simonetto[a,b], A. Tiko[a], M. Tosi[a,b], M. Zanetti[a,b], P. Zotto[a,b], A. Zucchetta[a,b], G. Zumerle[a,b]

INFN Sezione di Pavia [a], Università di Pavia [b], Pavia, Italy
A. Braghieri[a], D. Fiorina[a,b], P. Montagna[a,b], S.P. Ratti[a,b], V. Re[a], M. Ressegotti[a,b], C. Riccardi[a,b], P. Salvini[a], I. Vai[a], P. Vitulo[a,b]

INFN Sezione di Perugia [a], Università di Perugia [b], Perugia, Italy
M. Biasini[a,b], G.M. Bilei[a], D. Ciangottini[a,b], L. Fanò[a,b], P. Lariccia[a,b], R. Leonardi[a,b], E. Manoni[a], G. Mantovani[a,b], V. Mariani[a,b], M. Menichelli[a], A. Rossi[a,b], A. Santocchia[a,b], D. Spiga[a]

INFN Sezione di Pisa [a], Università di Pisa [b], Scuola Normale Superiore di Pisa [c], Pisa, Italy
K. Androsov[a], P. Azzurri[a], G. Bagliesi[a], V. Bertacchi[a,c], L. Bianchini[a], T. Boccali[a], R. Castaldi[a], M.A. Ciocci[a,b], R. Dell'Orso[a], S. Donato[a], L. Giannini[a,c], A. Giassi[a], M.T. Grippo[a], F. Ligabue[a,c], E. Manca[a,c], G. Mandorli[a,c], A. Messineo[a,b], F. Palla[a], A. Rizzi[a,b], G. Rolandi[32], S. Roy Chowdhury, A. Scribano[a], P. Spagnolo[a], R. Tenchini[a], G. Tonelli[a,b], N. Turini, A. Venturi[a], P.G. Verdini[a]

INFN Sezione di Roma [a], Sapienza Università di Roma [b], Rome, Italy
F. Cavallari[a], M. Cipriani[a,b], D. Del Re[a,b], E. Di Marco[a], M. Diemoz[a], E. Longo[a,b], P. Meridiani[a], G. Organtini[a,b], F. Pandolfi[a], R. Paramatti[a,b], C. Quaranta[a,b], S. Rahatlou[a,b], C. Rovelli[a], F. Santanastasio[a,b], L. Soffi[a,b]

INFN Sezione di Torino [a], Università di Torino [b], Torino, Italy, Università del Piemonte Orientale [c], Novara, Italy
N. Amapane[a,b], R. Arcidiacono[a,c], S. Argiro[a,b], M. Arneodo[a,c], N. Bartosik[a], R. Bellan[a,b], A. Bellora, C. Biino[a], A. Cappati[a,b], N. Cartiglia[a], S. Cometti[a], M. Costa[a,b], R. Covarelli[a,b], N. Demaria[a], B. Kiani[a,b], F. Legger, C. Mariotti[a], S. Maselli[a], E. Migliore[a,b], V. Monaco[a,b], E. Monteil[a,b], M. Monteno[a], M.M. Obertino[a,b], G. Ortona[a,b], L. Pacher[a,b], N. Pastrone[a], M. Pelliccioni[a], G.L. Pinna Angioni[a,b], A. Romero[a,b], M. Ruspa[a,c], R. Salvatico[a,b], V. Sola[a], A. Solano[a,b], D. Soldi[a,b], A. Staiano[a], D. Trocino[a,b]

INFN Sezione di Trieste [a], Università di Trieste [b], Trieste, Italy
S. Belforte[a], V. Candelise[a,b], M. Casarsa[a], F. Cossutti[a], A. Da Rold[a,b], G. Della Ricca[a,b], F. Vazzoler[a,b], A. Zanetti[a]

Kyungpook National University, Daegu, Korea
B. Kim, D.H. Kim, G.N. Kim, J. Lee, S.W. Lee, C.S. Moon, Y.D. Oh, S.I. Pak, S. Sekmen, D.C. Son, Y.C. Yang

Chonnam National University, Institute for Universe and Elementary Particles, Kwangju, Korea
H. Kim, D.H. Moon, G. Oh

Hanyang University, Seoul, Korea
B. Francois, T.J. Kim, J. Park

Korea University, Seoul, Korea
S. Cho, S. Choi, Y. Go, S. Ha, B. Hong, K. Lee, K.S. Lee, J. Lim, J. Park, S.K. Park, Y. Roh, J. Yoo

Kyung Hee University, Department of Physics
J. Goh

Sejong University, Seoul, Korea
H.S. Kim

Seoul National University, Seoul, Korea
J. Almond, J.H. Bhyun, J. Choi, S. Jeon, J. Kim, J.S. Kim, H. Lee, K. Lee, S. Lee, K. Nam, M. Oh, S.B. Oh, B.C. Radburn-Smith, U.K. Yang, H.D. Yoo, I. Yoon

University of Seoul, Seoul, Korea
D. Jeon, J.H. Kim, J.S.H. Lee, I.C. Park, I.J Watson

Sungkyunkwan University, Suwon, Korea
Y. Choi, C. Hwang, Y. Jeong, J. Lee, Y. Lee, I. Yu

Riga Technical University, Riga, Latvia
V. Veckalns[33]

Vilnius University, Vilnius, Lithuania
V. Dudenas, A. Juodagalvis, A. Rinkevicius, G. Tamulaitis, J. Vaitkus

National Centre for Particle Physics, Universiti Malaya, Kuala Lumpur, Malaysia
F. Mohamad Idris[34], W.A.T. Wan Abdullah, M.N. Yusli, Z. Zolkapli

Universidad de Sonora (UNISON), Hermosillo, Mexico
J.F. Benitez, A. Castaneda Hernandez, J.A. Murillo Quijada, L. Valencia Palomo

Centro de Investigacion y de Estudios Avanzados del IPN, Mexico City, Mexico
H. Castilla-Valdez, E. De La Cruz-Burelo, I. Heredia-De La Cruz[35], R. Lopez-Fernandez, A. Sanchez-Hernandez

Universidad Iberoamericana, Mexico City, Mexico
S. Carrillo Moreno, C. Oropeza Barrera, M. Ramirez-Garcia, F. Vazquez Valencia

Benemerita Universidad Autonoma de Puebla, Puebla, Mexico
J. Eysermans, I. Pedraza, H.A. Salazar Ibarguen, C. Uribe Estrada

Universidad Autónoma de San Luis Potosí, San Luis Potosí, Mexico
A. Morelos Pineda

University of Montenegro, Podgorica, Montenegro
J. Mijuskovic[2], N. Raicevic

University of Auckland, Auckland, New Zealand
D. Krofcheck

University of Canterbury, Christchurch, New Zealand
S. Bheesette, P.H. Butler, P. Lujan

National Centre for Physics, Quaid-I-Azam University, Islamabad, Pakistan
A. Ahmad, M. Ahmad, M.I.M. Awan, Q. Hassan, H.R. Hoorani, W.A. Khan, M.A. Shah, M. Shoaib, M. Waqas

AGH University of Science and Technology Faculty of Computer Science, Electronics and Telecommunications, Krakow, Poland
V. Avati, L. Grzanka, M. Malawski

National Centre for Nuclear Research, Swierk, Poland
H. Bialkowska, M. Bluj, B. Boimska, M. Górski, M. Kazana, M. Szleper, P. Zalewski

Institute of Experimental Physics, Faculty of Physics, University of Warsaw, Warsaw, Poland
K. Bunkowski, A. Byszuk[36], K. Doroba, A. Kalinowski, M. Konecki, J. Krolikowski, M. Olszewski, M. Walczak

Laboratório de Instrumentação e Física Experimental de Partículas, Lisboa, Portugal
M. Araujo, P. Bargassa, D. Bastos, A. Di Francesco, P. Faccioli, B. Galinhas, M. Gallinaro, J. Hollar, N. Leonardo, T. Niknejad, J. Seixas, K. Shchelina, G. Strong, O. Toldaiev, J. Varela

Joint Institute for Nuclear Research, Dubna, Russia
S. Afanasiev, P. Bunin, M. Gavrilenko, I. Golutvin, I. Gorbunov, A. Kamenev, V. Karjavine, A. Lanev, A. Malakhov, V. Matveev[37,38], P. Moisenz, V. Palichik, V. Perelygin, M. Savina, S. Shmatov, S. Shulha, N. Skatchkov, V. Smirnov, N. Voytishin, A. Zarubin

Petersburg Nuclear Physics Institute, Gatchina (St. Petersburg), Russia
L. Chtchipounov, V. Golovtcov, Y. Ivanov, V. Kim[39], E. Kuznetsova[40], P. Levchenko, V. Murzin, V. Oreshkin, I. Smirnov, D. Sosnov, V. Sulimov, L. Uvarov, A. Vorobyev

Institute for Nuclear Research, Moscow, Russia
Yu. Andreev, A. Dermenev, S. Gninenko, N. Golubev, A. Karneyeu, M. Kirsanov, N. Krasnikov, A. Pashenkov, D. Tlisov, A. Toropin

Institute for Theoretical and Experimental Physics named by A.I. Alikhanov of NRC 'Kurchatov Institute', Moscow, Russia
V. Epshteyn, V. Gavrilov, N. Lychkovskaya, A. Nikitenko[41], V. Popov, I. Pozdnyakov, G. Safronov, A. Spiridonov, A. Stepennov, M. Toms, E. Vlasov, A. Zhokin

Moscow Institute of Physics and Technology, Moscow, Russia
T. Aushev

National Research Nuclear University 'Moscow Engineering Physics Institute' (MEPhI), Moscow, Russia
O. Bychkova, R. Chistov[42], M. Danilov[42], S. Polikarpov[42], E. Tarkovskii

P.N. Lebedev Physical Institute, Moscow, Russia
V. Andreev, M. Azarkin, I. Dremin, M. Kirakosyan, A. Terkulov

Skobeltsyn Institute of Nuclear Physics, Lomonosov Moscow State University, Moscow, Russia
A. Baskakov, A. Belyaev, E. Boos, V. Bunichev, M. Dubinin[43], L. Dudko, A. Gribushin, V. Klyukhin, O. Kodolova, I. Lokhtin, S. Obraztsov, S. Petrushanko, V. Savrin

Novosibirsk State University (NSU), Novosibirsk, Russia
A. Barnyakov[44], V. Blinov[44], T. Dimova[44], L. Kardapoltsev[44], Y. Skovpen[44]

Institute for High Energy Physics of National Research Centre 'Kurchatov Institute', Protvino, Russia
I. Azhgirey, I. Bayshev, S. Bitioukov, V. Kachanov, D. Konstantinov, P. Mandrik, V. Petrov, R. Ryutin, S. Slabospitskii, A. Sobol, S. Troshin, N. Tyurin, A. Uzunian, A. Volkov

National Research Tomsk Polytechnic University, Tomsk, Russia
A. Babaev, A. Iuzhakov, V. Okhotnikov

Tomsk State University, Tomsk, Russia
V. Borchsh, V. Ivanchenko, E. Tcherniaev

University of Belgrade: Faculty of Physics and VINCA Institute of Nuclear Sciences
P. Adzic[45], P. Cirkovic, M. Dordevic, P. Milenovic, J. Milosevic, M. Stojanovic

Centro de Investigaciones Energéticas Medioambientales y Tecnológicas (CIEMAT), Madrid, Spain
M. Aguilar-Benitez, J. Alcaraz Maestre, A. Álvarez Fernández, I. Bachiller, M. Barrio Luna, CristinaF. Bedoya, J.A. Brochero Cifuentes, C.A. Carrillo Montoya, M. Cepeda, M. Cerrada, N. Colino, B. De La Cruz, A. Delgado Peris, J.P. Fernández Ramos, J. Flix, M.C. Fouz, O. Gonzalez Lopez, S. Goy Lopez, J.M. Hernandez, M.I. Josa, D. Moran, Á. Navarro Tobar, A. Pérez-Calero Yzquierdo, J. Puerta Pelayo, I. Redondo, L. Romero, S. Sánchez Navas, M.S. Soares, A. Triossi, C. Willmott

Universidad Autónoma de Madrid, Madrid, Spain
C. Albajar, J.F. de Trocóniz, R. Reyes-Almanza

Universidad de Oviedo, Instituto Universitario de Ciencias y Tecnologías Espaciales de Asturias (ICTEA), Oviedo, Spain
B. Alvarez Gonzalez, J. Cuevas, C. Erice, J. Fernandez Menendez, S. Folgueras, I. Gonzalez Caballero, J.R. González Fernández, E. Palencia Cortezon, C. Ramón Álvarez, V. Rodríguez Bouza, S. Sanchez Cruz

Instituto de Física de Cantabria (IFCA), CSIC-Universidad de Cantabria, Santander, Spain
I.J. Cabrillo, A. Calderon, B. Chazin Quero, J. Duarte Campderros, M. Fernandez, P.J. Fernández Manteca, A. García Alonso, G. Gomez, C. Martinez Rivero, P. Martinez Ruiz del Arbol, F. Matorras, J. Piedra Gomez, C. Prieels, F. Ricci-Tam, T. Rodrigo, A. Ruiz-Jimeno, L. Russo[46], L. Scodellaro, I. Vila, J.M. Vizan Garcia

University of Colombo, Colombo, Sri Lanka
D.U.J. Sonnadara

University of Ruhuna, Department of Physics, Matara, Sri Lanka
W.G.D. Dharmaratna, N. Wickramage

CERN, European Organization for Nuclear Research, Geneva, Switzerland
D. Abbaneo, B. Akgun, E. Auffray, G. Auzinger, J. Baechler, P. Baillon, A.H. Ball, D. Barney, J. Bendavid, M. Bianco, A. Bocci, P. Bortignon, E. Bossini, E. Brondolin, T. Camporesi, A. Caratelli, G. Cerminara, E. Chapon, G. Cucciati, D. d'Enterria, A. Dabrowski, N. Daci, V. Daponte, A. David, O. Davignon, A. De Roeck, M. Deile, R. Di Maria, M. Dobson, M. Dünser, N. Dupont, A. Elliott-Peisert, N. Emriskova, F. Fallavollita[47], D. Fasanella, S. Fiorendi, G. Franzoni, J. Fulcher, W. Funk, S. Giani, D. Gigi, K. Gill, F. Glege, L. Gouskos, M. Gruchala, M. Guilbaud, D. Gulhan, J. Hegeman, C. Heidegger, Y. Iiyama, V. Innocente, T. James, P. Janot, O. Karacheban[19], J. Kaspar, J. Kieseler, M. Krammer[1], N. Kratochwil, C. Lange, P. Lecoq, K. Long, C. Lourenço, L. Malgeri, M. Mannelli, A. Massironi, F. Meijers, S. Mersi, E. Meschi, F. Moortgat, M. Mulders, J. Ngadiuba, J. Niedziela, S. Nourbakhsh, S. Orfanelli, L. Orsini, F. Pantaleo[16], L. Pape, E. Perez, M. Peruzzi, A. Petrilli, G. Petrucciani, A. Pfeiffer, M. Pierini, F.M. Pitters, D. Rabady, A. Racz, M. Rieger, M. Rovere, H. Sakulin, J. Salfeld-Nebgen, S. Scarfi, C. Schäfer, C. Schwick, M. Selvaggi, A. Sharma, P. Silva, W. Snoeys, P. Sphicas[48], J. Steggemann, S. Summers, V.R. Tavolaro, D. Treille, A. Tsirou, G.P. Van Onsem, A. Vartak, M. Verzetti, W.D. Zeuner

Paul Scherrer Institut, Villigen, Switzerland
L. Caminada[49], K. Deiters, W. Erdmann, R. Horisberger, Q. Ingram, H.C. Kaestli, D. Kotlinski, U. Langenegger, T. Rohe

ETH Zurich - Institute for Particle Physics and Astrophysics (IPA), Zurich, Switzerland
M. Backhaus, P. Berger, N. Chernyavskaya, G. Dissertori, M. Dittmar, M. Donegà, C. Dorfer, T.A. Gómez Espinosa, C. Grab, D. Hits, W. Lustermann, R.A. Manzoni, M.T. Meinhard, F. Micheli, P. Musella, F. Nessi-Tedaldi, F. Pauss, G. Perrin, L. Perrozzi, S. Pigazzini, M.G. Ratti, M. Reichmann, C. Reissel, T. Reitenspiess, B. Ristic, D. Ruini, D.A. Sanz Becerra, M. Schönenberger, L. Shchutska, M.L. Vesterbacka Olsson, R. Wallny, D.H. Zhu

Universität Zürich, Zurich, Switzerland
T.K. Aarrestad, C. Amsler[50], C. Botta, D. Brzhechko, M.F. Canelli, A. De Cosa, R. Del Burgo, B. Kilminster, S. Leontsinis, V.M. Mikuni, I. Neutelings, G. Rauco, P. Robmann, K. Schweiger, Y. Takahashi, S. Wertz

National Central University, Chung-Li, Taiwan
C.M. Kuo, W. Lin, A. Roy, S.S. Yu

National Taiwan University (NTU), Taipei, Taiwan
P. Chang, Y. Chao, K.F. Chen, P.H. Chen, W.-S. Hou, Y.y. Li, R.-S. Lu, E. Paganis, A. Psallidas, A. Steen

Chulalongkorn University, Faculty of Science, Department of Physics, Bangkok, Thailand
B. Asavapibhop, C. Asawatangtrakuldee, N. Srimanobhas, N. Suwonjandee

Çukurova University, Physics Department, Science and Art Faculty, Adana, Turkey
A. Bat, F. Boran, A. Celik[51], S. Damarseckin[52], Z.S. Demiroglu, F. Dolek, C. Dozen[53], I. Dumanoglu[54], G. Gokbulut, EmineGurpinar Guler[55], Y. Guler, I. Hos[56], C. Isik, E.E. Kangal[57], O. Kara, A. Kayis Topaksu, U. Kiminsu, G. Onengut, K. Ozdemir[58], S. Ozturk[59], A.E. Simsek, U.G. Tok, S. Turkcapar, I.S. Zorbakir, C. Zorbilmez

Middle East Technical University, Physics Department, Ankara, Turkey
B. Isildak[60], G. Karapinar[61], M. Yalvac[62]

Bogazici University, Istanbul, Turkey
I.O. Atakisi, E. Gülmez, M. Kaya[63], O. Kaya[64], Ö. Özçelik, S. Tekten, E.A. Yetkin[65]

Istanbul Technical University, Istanbul, Turkey
A. Cakir, K. Cankocak[54], Y. Komurcu, S. Sen[66]

Istanbul University, Istanbul, Turkey
S. Cerci[67], B. Kaynak, S. Ozkorucuklu, D. Sunar Cerci[67]

Institute for Scintillation Materials of National Academy of Science of Ukraine, Kharkov, Ukraine
B. Grynyov

National Scientific Center, Kharkov Institute of Physics and Technology, Kharkov, Ukraine
L. Levchuk

University of Bristol, Bristol, United Kingdom
E. Bhal, S. Bologna, J.J. Brooke, D. Burns[68], E. Clement, D. Cussans, H. Flacher, J. Goldstein, G.P. Heath, H.F. Heath, L. Kreczko, B. Krikler, S. Paramesvaran, T. Sakuma, S. Seif El Nasr-Storey, V.J. Smith, J. Taylor, A. Titterton

Rutherford Appleton Laboratory, Didcot, United Kingdom
K.W. Bell, A. Belyaev[69], C. Brew, R.M. Brown, D.J.A. Cockerill, J.A. Coughlan, K. Harder, S. Harper, J. Linacre, K. Manolopoulos, D.M. Newbold, E. Olaiya, D. Petyt, T. Reis, T. Schuh, C.H. Shepherd-Themistocleous, A. Thea, I.R. Tomalin, T. Williams

Imperial College, London, United Kingdom
R. Bainbridge, P. Bloch, S. Bonomally, J. Borg, S. Breeze, O. Buchmuller, A. Bundock, GurpreetSingh CHAHAL[70], D. Colling, P. Dauncey, G. Davies, M. Della Negra, P. Everaerts, G. Hall, G. Iles, M. Komm, L. Lyons, A.-M. Magnan, S. Malik, A. Martelli, V. Milosevic, A. Morton, J. Nash[71], V. Palladino, M. Pesaresi, D.M. Raymond, A. Richards, A. Rose, E. Scott, C. Seez, A. Shtipliyski, M. Stoye, T. Strebler, A. Tapper, K. Uchida, T. Virdee[16], N. Wardle, D. Winterbottom, A.G. Zecchinelli, S.C. Zenz

Brunel University, Uxbridge, United Kingdom
J.E. Cole, P.R. Hobson, A. Khan, P. Kyberd, C.K. Mackay, I.D. Reid, L. Teodorescu, S. Zahid

Baylor University, Waco, USA
A. Brinkerhoff, K. Call, B. Caraway, J. Dittmann, K. Hatakeyama, C. Madrid, B. McMaster, N. Pastika, C. Smith

Catholic University of America, Washington, DC, USA
R. Bartek, A. Dominguez, R. Uniyal, A.M. Vargas Hernandez

The University of Alabama, Tuscaloosa, USA
A. Buccilli, S.I. Cooper, S.V. Gleyzer, C. Henderson, P. Rumerio, C. West

Boston University, Boston, USA
A. Albert, D. Arcaro, Z. Demiragli, D. Gastler, C. Richardson, J. Rohlf, D. Sperka, D. Spitzbart, I. Suarez, L. Sulak, D. Zou

Brown University, Providence, USA
G. Benelli, B. Burkle, X. Coubez[17], D. Cutts, Y.t. Duh, M. Hadley, U. Heintz, J.M. Hogan[72], K.H.M. Kwok, E. Laird, G. Landsberg, K.T. Lau, J. Lee, M. Narain, S. Sagir[73], R. Syarif, E. Usai, W.Y. Wong, D. Yu, W. Zhang

University of California, Davis, Davis, USA
R. Band, C. Brainerd, R. Breedon, M. Calderon De La Barca Sanchez, M. Chertok, J. Conway, R. Conway, P.T. Cox, R. Erbacher, C. Flores, G. Funk, F. Jensen, W. Ko[†], O. Kukral, R. Lander, M. Mulhearn, D. Pellett, J. Pilot, M. Shi, D. Taylor, K. Tos, M. Tripathi, Z. Wang, F. Zhang

University of California, Los Angeles, USA
M. Bachtis, C. Bravo, R. Cousins, A. Dasgupta, A. Florent, J. Hauser, M. Ignatenko, N. Mccoll, W.A. Nash, S. Regnard, D. Saltzberg, C. Schnaible, B. Stone, V. Valuev

University of California, Riverside, Riverside, USA
K. Burt, Y. Chen, R. Clare, J.W. Gary, S.M.A. Ghiasi Shirazi, G. Hanson, G. Karapostoli, O.R. Long, N. Manganelli, M. Olmedo Negrete, M.I. Paneva, W. Si, S. Wimpenny, B.R. Yates, Y. Zhang

University of California, San Diego, La Jolla, USA
J.G. Branson, P. Chang, S. Cittolin, S. Cooperstein, N. Deelen, M. Derdzinski, J. Duarte, R. Gerosa, D. Gilbert, B. Hashemi, D. Klein, V. Krutelyov, J. Letts, M. Masciovecchio, S. May, S. Padhi, M. Pieri, V. Sharma, M. Tadel, F. Würthwein, A. Yagil, G. Zevi Della Porta

University of California, Santa Barbara - Department of Physics, Santa Barbara, USA
N. Amin, R. Bhandari, C. Campagnari, M. Citron, V. Dutta, J. Incandela, B. Marsh, H. Mei, A. Ovcharova, H. Qu, J. Richman, U. Sarica, D. Stuart, S. Wang

California Institute of Technology, Pasadena, USA
D. Anderson, A. Bornheim, O. Cerri, I. Dutta, J.M. Lawhorn, N. Lu, J. Mao, H.B. Newman, T.Q. Nguyen, J. Pata, M. Spiropulu, J.R. Vlimant, S. Xie, Z. Zhang, R.Y. Zhu

Carnegie Mellon University, Pittsburgh, USA
M.B. Andrews, T. Ferguson, T. Mudholkar, M. Paulini, M. Sun, I. Vorobiev, M. Weinberg

University of Colorado Boulder, Boulder, USA
J.P. Cumalat, W.T. Ford, E. MacDonald, T. Mulholland, R. Patel, A. Perloff, K. Stenson, K.A. Ulmer, S.R. Wagner

Cornell University, Ithaca, USA
J. Alexander, Y. Cheng, J. Chu, A. Datta, A. Frankenthal, K. Mcdermott, J.R. Patterson, D. Quach, A. Ryd, S.M. Tan, Z. Tao, J. Thom, P. Wittich, M. Zientek

Fermi National Accelerator Laboratory, Batavia, USA
S. Abdullin, M. Albrow, M. Alyari, G. Apollinari, A. Apresyan, A. Apyan, S. Banerjee, L.A.T. Bauerdick, A. Beretvas, D. Berry, J. Berryhill, P.C. Bhat, K. Burkett, J.N. Butler, A. Canepa, G.B. Cerati, H.W.K. Cheung, F. Chlebana, M. Cremonesi, V.D. Elvira, J. Freeman, Z. Gecse, E. Gottschalk, L. Gray, D. Green, S. Grünendahl, O. Gutsche, J. Hanlon, R.M. Harris, S. Hasegawa, R. Heller, J. Hirschauer, B. Jayatilaka, S. Jindariani, M. Johnson, U. Joshi, T. Klijnsma, B. Klima, M.J. Kortelainen, B. Kreis, S. Lammel, J. Lewis, D. Lincoln, R. Lipton, M. Liu, T. Liu, J. Lykken, K. Maeshima, J.M. Marraffino, D. Mason, P. McBride,

P. Merkel, S. Mrenna, S. Nahn, V. O'Dell, V. Papadimitriou, K. Pedro, C. Pena[43], F. Ravera, A. Reinsvold Hall, L. Ristori, B. Schneider, E. Sexton-Kennedy, N. Smith, A. Soha, W.J. Spalding, L. Spiegel, S. Stoynev, J. Strait, L. Taylor, S. Tkaczyk, N.V. Tran, L. Uplegger, E.W. Vaandering, C. Vernieri, R. Vidal, M. Wang, H.A. Weber, A. Woodard

University of Florida, Gainesville, USA
D. Acosta, P. Avery, D. Bourilkov, L. Cadamuro, V. Cherepanov, F. Errico, R.D. Field, D. Guerrero, B.M. Joshi, M. Kim, J. Konigsberg, A. Korytov, K.H. Lo, K. Matchev, N. Menendez, G. Mitselmakher, D. Rosenzweig, K. Shi, J. Wang, S. Wang, X. Zuo

Florida International University, Miami, USA
Y.R. Joshi

Florida State University, Tallahassee, USA
T. Adams, A. Askew, S. Hagopian, V. Hagopian, K.F. Johnson, R. Khurana, T. Kolberg, G. Martinez, T. Perry, H. Prosper, C. Schiber, R. Yohay, J. Zhang

Florida Institute of Technology, Melbourne, USA
M.M. Baarmand, M. Hohlmann, D. Noonan, M. Rahmani, M. Saunders, F. Yumiceva

University of Illinois at Chicago (UIC), Chicago, USA
M.R. Adams, L. Apanasevich, R.R. Betts, R. Cavanaugh, X. Chen, S. Dittmer, O. Evdokimov, C.E. Gerber, D.A. Hangal, D.J. Hofman, V. Kumar, C. Mills, T. Roy, M.B. Tonjes, N. Varelas, J. Viinikainen, H. Wang, X. Wang, Z. Wu

The University of Iowa, Iowa City, USA
M. Alhusseini, B. Bilki[55], K. Dilsiz[74], S. Durgut, R.P. Gandrajula, M. Haytmyradov, V. Khristenko, O.K. Köseyan, J.-P. Merlo, A. Mestvirishvili[75], A. Moeller, J. Nachtman, H. Ogul[76], Y. Onel, F. Ozok[77], A. Penzo, C. Snyder, E. Tiras, J. Wetzel, K. Yi[78]

Johns Hopkins University, Baltimore, USA
B. Blumenfeld, A. Cocoros, N. Eminizer, A.V. Gritsan, W.T. Hung, S. Kyriacou, P. Maksimovic, J. Roskes, M. Swartz, T.Á. Vámi

The University of Kansas, Lawrence, USA
C. Baldenegro Barrera, P. Baringer, A. Bean, S. Boren, A. Bylinkin, T. Isidori, S. Khalil, J. King, G. Krintiras, A. Kropivnitskaya, C. Lindsey, D. Majumder, W. Mcbrayer, N. Minafra, M. Murray, C. Rogan, C. Royon, S. Sanders, E. Schmitz, J.D. Tapia Takaki, Q. Wang, J. Williams, G. Wilson

Kansas State University, Manhattan, USA
S. Duric, A. Ivanov, K. Kaadze, D. Kim, Y. Maravin, D.R. Mendis, T. Mitchell, A. Modak, A. Mohammadi

Lawrence Livermore National Laboratory, Livermore, USA
F. Rebassoo, D. Wright

University of Maryland, College Park, USA
A. Baden, O. Baron, A. Belloni, S.C. Eno, Y. Feng, N.J. Hadley, S. Jabeen, G.Y. Jeng, R.G. Kellogg, A.C. Mignerey, S. Nabili, M. Seidel, Y.H. Shin, A. Skuja, S.C. Tonwar, L. Wang, K. Wong

Massachusetts Institute of Technology, Cambridge, USA
D. Abercrombie, B. Allen, R. Bi, S. Brandt, W. Busza, I.A. Cali, M. D'Alfonso, G. Gomez Ceballos, M. Goncharov, P. Harris, D. Hsu, M. Hu, M. Klute, D. Kovalskyi, Y.-J. Lee, P.D. Luckey, B. Maier, A.C. Marini, C. Mcginn, C. Mironov, S. Narayanan, X. Niu, C. Paus,

D. Rankin, C. Roland, G. Roland, Z. Shi, G.S.F. Stephans, K. Sumorok, K. Tatar, D. Velicanu, J. Wang, T.W. Wang, B. Wyslouch

University of Minnesota, Minneapolis, USA
R.M. Chatterjee, A. Evans, S. Guts†, P. Hansen, J. Hiltbrand, Sh. Jain, Y. Kubota, Z. Lesko, J. Mans, M. Revering, R. Rusack, R. Saradhy, N. Schroeder, N. Strobbe, M.A. Wadud

University of Mississippi, Oxford, USA
J.G. Acosta, S. Oliveros

University of Nebraska-Lincoln, Lincoln, USA
K. Bloom, S. Chauhan, D.R. Claes, C. Fangmeier, L. Finco, F. Golf, R. Kamalieddin, I. Kravchenko, J.E. Siado, G.R. Snow†, B. Stieger, W. Tabb

State University of New York at Buffalo, Buffalo, USA
G. Agarwal, C. Harrington, I. Iashvili, A. Kharchilava, C. McLean, D. Nguyen, A. Parker, J. Pekkanen, S. Rappoccio, B. Roozbahani

Northeastern University, Boston, USA
G. Alverson, E. Barberis, C. Freer, Y. Haddad, A. Hortiangtham, G. Madigan, B. Marzocchi, D.M. Morse, T. Orimoto, L. Skinnari, A. Tishelman-Charny, T. Wamorkar, B. Wang, A. Wisecarver, D. Wood

Northwestern University, Evanston, USA
S. Bhattacharya, J. Bueghly, G. Fedi, A. Gilbert, T. Gunter, K.A. Hahn, N. Odell, M.H. Schmitt, K. Sung, M. Velasco

University of Notre Dame, Notre Dame, USA
R. Bucci, N. Dev, R. Goldouzian, M. Hildreth, K. Hurtado Anampa, C. Jessop, D.J. Karmgard, K. Lannon, W. Li, N. Loukas, N. Marinelli, I. Mcalister, F. Meng, Y. Musienko[37], R. Ruchti, P. Siddireddy, G. Smith, S. Taroni, M. Wayne, A. Wightman, M. Wolf

The Ohio State University, Columbus, USA
J. Alimena, B. Bylsma, L.S. Durkin, B. Francis, C. Hill, W. Ji, A. Lefeld, T.Y. Ling, B.L. Winer

Princeton University, Princeton, USA
G. Dezoort, P. Elmer, J. Hardenbrook, N. Haubrich, S. Higginbotham, A. Kalogeropoulos, S. Kwan, D. Lange, M.T. Lucchini, J. Luo, D. Marlow, K. Mei, I. Ojalvo, J. Olsen, C. Palmer, P. Piroué, D. Stickland, C. Tully

University of Puerto Rico, Mayaguez, USA
S. Malik, S. Norberg

Purdue University, West Lafayette, USA
A. Barker, V.E. Barnes, R. Chawla, S. Das, L. Gutay, M. Jones, A.W. Jung, B. Mahakud, D.H. Miller, G. Negro, N. Neumeister, C.C. Peng, S. Piperov, H. Qiu, J.F. Schulte, N. Trevisani, F. Wang, R. Xiao, W. Xie

Purdue University Northwest, Hammond, USA
T. Cheng, J. Dolen, N. Parashar

Rice University, Houston, USA
A. Baty, U. Behrens, S. Dildick, K.M. Ecklund, S. Freed, F.J.M. Geurts, M. Kilpatrick, Arun Kumar, W. Li, B.P. Padley, R. Redjimi, J. Roberts, J. Rorie, W. Shi, A.G. Stahl Leiton, Z. Tu, A. Zhang

University of Rochester, Rochester, USA
A. Bodek, P. de Barbaro, R. Demina, J.L. Dulemba, C. Fallon, T. Ferbel, M. Galanti, A. Garcia-Bellido, O. Hindrichs, A. Khukhunaishvili, E. Ranken, R. Taus

Rutgers, The State University of New Jersey, Piscataway, USA
B. Chiarito, J.P. Chou, A. Gandrakota, Y. Gershtein, E. Halkiadakis, A. Hart, M. Heindl, E. Hughes, S. Kaplan, I. Laflotte, A. Lath, R. Montalvo, K. Nash, M. Osherson, S. Salur, S. Schnetzer, S. Somalwar, R. Stone, S. Thomas

University of Tennessee, Knoxville, USA
H. Acharya, A.G. Delannoy, S. Spanier

Texas A&M University, College Station, USA
O. Bouhali[79], M. Dalchenko, M. De Mattia, A. Delgado, R. Eusebi, J. Gilmore, T. Huang, T. Kamon[80], H. Kim, S. Luo, S. Malhotra, D. Marley, R. Mueller, D. Overton, L. Perniè, D. Rathjens, A. Safonov

Texas Tech University, Lubbock, USA
N. Akchurin, J. Damgov, F. De Guio, V. Hegde, S. Kunori, K. Lamichhane, S.W. Lee, T. Mengke, S. Muthumuni, T. Peltola, S. Undleeb, I. Volobouev, Z. Wang, A. Whitbeck

Vanderbilt University, Nashville, USA
S. Greene, A. Gurrola, R. Janjam, W. Johns, C. Maguire, A. Melo, H. Ni, K. Padeken, F. Romeo, P. Sheldon, S. Tuo, J. Velkovska, M. Verweij

University of Virginia, Charlottesville, USA
M.W. Arenton, P. Barria, B. Cox, G. Cummings, J. Hakala, R. Hirosky, M. Joyce, A. Ledovskoy, C. Neu, B. Tannenwald, Y. Wang, E. Wolfe, F. Xia

Wayne State University, Detroit, USA
R. Harr, P.E. Karchin, N. Poudyal, J. Sturdy, P. Thapa

University of Wisconsin - Madison, Madison, WI, USA
K. Black, T. Bose, J. Buchanan, C. Caillol, D. Carlsmith, S. Dasu, I. De Bruyn, L. Dodd, C. Galloni, H. He, M. Herndon, A. Hervé, U. Hussain, A. Lanaro, A. Loeliger, R. Loveless, J. Madhusudanan Sreekala, A. Mallampalli, D. Pinna, T. Ruggles, A. Savin, V. Sharma, W.H. Smith, D. Teague, S. Trembath-reichert

†: Deceased
1: Also at Vienna University of Technology, Vienna, Austria
2: Also at IRFU, CEA, Université Paris-Saclay, Gif-sur-Yvette, France
3: Also at Universidade Estadual de Campinas, Campinas, Brazil
4: Also at Federal University of Rio Grande do Sul, Porto Alegre, Brazil
5: Also at UFMS, Nova Andradina, Brazil
6: Also at Universidade Federal de Pelotas, Pelotas, Brazil
7: Also at Université Libre de Bruxelles, Bruxelles, Belgium
8: Also at University of Chinese Academy of Sciences, Beijing, China
9: Also at Institute for Theoretical and Experimental Physics named by A.I. Alikhanov of NRC 'Kurchatov Institute', Moscow, Russia
10: Also at Joint Institute for Nuclear Research, Dubna, Russia
11: Also at Cairo University, Cairo, Egypt
12: Now at British University in Egypt, Cairo, Egypt
13: Also at Purdue University, West Lafayette, USA
14: Also at Université de Haute Alsace, Mulhouse, France

15: Also at Erzincan Binali Yildirim University, Erzincan, Turkey
16: Also at CERN, European Organization for Nuclear Research, Geneva, Switzerland
17: Also at RWTH Aachen University, III. Physikalisches Institut A, Aachen, Germany
18: Also at University of Hamburg, Hamburg, Germany
19: Also at Brandenburg University of Technology, Cottbus, Germany
20: Also at Institute of Physics, University of Debrecen, Debrecen, Hungary, Debrecen, Hungary
21: Also at Institute of Nuclear Research ATOMKI, Debrecen, Hungary
22: Also at MTA-ELTE Lendület CMS Particle and Nuclear Physics Group, Eötvös Loránd University, Budapest, Hungary, Budapest, Hungary
23: Also at IIT Bhubaneswar, Bhubaneswar, India, Bhubaneswar, India
24: Also at Institute of Physics, Bhubaneswar, India
25: Also at G.H.G. Khalsa College, Punjab, India
26: Also at Shoolini University, Solan, India
27: Also at University of Hyderabad, Hyderabad, India
28: Also at University of Visva-Bharati, Santiniketan, India
29: Now at INFN Sezione di Bari [a], Università di Bari [b], Politecnico di Bari [c], Bari, Italy
30: Also at Italian National Agency for New Technologies, Energy and Sustainable Economic Development, Bologna, Italy
31: Also at Centro Siciliano di Fisica Nucleare e di Struttura Della Materia, Catania, Italy
32: Also at Scuola Normale e Sezione dell'INFN, Pisa, Italy
33: Also at Riga Technical University, Riga, Latvia, Riga, Latvia
34: Also at Malaysian Nuclear Agency, MOSTI, Kajang, Malaysia
35: Also at Consejo Nacional de Ciencia y Tecnología, Mexico City, Mexico
36: Also at Warsaw University of Technology, Institute of Electronic Systems, Warsaw, Poland
37: Also at Institute for Nuclear Research, Moscow, Russia
38: Now at National Research Nuclear University 'Moscow Engineering Physics Institute' (MEPhI), Moscow, Russia
39: Also at St. Petersburg State Polytechnical University, St. Petersburg, Russia
40: Also at University of Florida, Gainesville, USA
41: Also at Imperial College, London, United Kingdom
42: Also at P.N. Lebedev Physical Institute, Moscow, Russia
43: Also at California Institute of Technology, Pasadena, USA
44: Also at Budker Institute of Nuclear Physics, Novosibirsk, Russia
45: Also at Faculty of Physics, University of Belgrade, Belgrade, Serbia
46: Also at Università degli Studi di Siena, Siena, Italy
47: Also at INFN Sezione di Pavia [a], Università di Pavia [b], Pavia, Italy, Pavia, Italy
48: Also at National and Kapodistrian University of Athens, Athens, Greece
49: Also at Universität Zürich, Zurich, Switzerland
50: Also at Stefan Meyer Institute for Subatomic Physics, Vienna, Austria, Vienna, Austria
51: Also at Burdur Mehmet Akif Ersoy University, BURDUR, Turkey
52: Also at Şırnak University, Sirnak, Turkey
53: Also at Department of Physics, Tsinghua University, Beijing, China, Beijing, China
54: Also at Near East University, Research Center of Experimental Health Science, Nicosia, Turkey
55: Also at Beykent University, Istanbul, Turkey, Istanbul, Turkey
56: Also at Istanbul Aydin University, Application and Research Center for Advanced Studies (App. & Res. Cent. for Advanced Studies), Istanbul, Turkey
57: Also at Mersin University, Mersin, Turkey

58: Also at Piri Reis University, Istanbul, Turkey
59: Also at Gaziosmanpasa University, Tokat, Turkey
60: Also at Ozyegin University, Istanbul, Turkey
61: Also at Izmir Institute of Technology, Izmir, Turkey
62: Also at Bozok Universitetesi Rektörlügü, Yozgat, Turkey
63: Also at Marmara University, Istanbul, Turkey
64: Also at Kafkas University, Kars, Turkey
65: Also at Istanbul Bilgi University, Istanbul, Turkey
66: Also at Hacettepe University, Ankara, Turkey
67: Also at Adiyaman University, Adiyaman, Turkey
68: Also at Vrije Universiteit Brussel, Brussel, Belgium
69: Also at School of Physics and Astronomy, University of Southampton, Southampton, United Kingdom
70: Also at IPPP Durham University, Durham, United Kingdom
71: Also at Monash University, Faculty of Science, Clayton, Australia
72: Also at Bethel University, St. Paul, Minneapolis, USA, St. Paul, USA
73: Also at Karamanoğlu Mehmetbey University, Karaman, Turkey
74: Also at Bingol University, Bingol, Turkey
75: Also at Georgian Technical University, Tbilisi, Georgia
76: Also at Sinop University, Sinop, Turkey
77: Also at Mimar Sinan University, Istanbul, Istanbul, Turkey
78: Also at Nanjing Normal University Department of Physics, Nanjing, China
79: Also at Texas A&M University at Qatar, Doha, Qatar
80: Also at Kyungpook National University, Daegu, Korea, Daegu, Korea